5 Oil Spill Source Identification by Comprehensive Two-Dimensional Gas Chromatography (GC × GC)

Richard B. Gaines,[1] Glenn S. Frysinger,[1] Christopher M. Reddy,[2] and Robert K. Nelson[2]

[1]U.S. Coast Guard Academy, 27 Mohegan Ave., New London, CT, 06320.
[2]Woods Hole Oceanographic Institute, Department of Marine Chemistry and Geochemistry, 360 Woods Hole Rd., Woods Hole, MA 02543.

5.1 Introduction

5.1.1 The Need for High-Resolution Separations

Petroleum is a complex mixture containing thousands of compounds with different chemical functionality including alkanes, one- and multi-ring cycloalkanes, one- and multi-ring aromatics, and compounds containing sulfur, oxygen, and nitrogen. Detailed studies of the source, fate, and transport of petroleum spills in the environment often require high-resolution separations of target compounds and classes of compounds from the rest of the complex mixture. Routine one-dimensional chromatographic methods fall far short of the resolving power required due to the random nature of chromatogram peak spacing. For example, a peak capacity of 100 is needed to separate 100 evenly spaced peaks. Evenly spaced peaks can be expected for simple mixtures such as homologous series of normal alkanes, but if greater chemical diversity is present in the sample, randomly distributed peaks are likely. Statistics show that to separate 98 out of 100 randomly distributed peaks, a peak capacity of 10,000 is required (Davis et al., 1994). Therefore, samples with hundreds or thousands of compounds cannot be resolved using a single chromatographic column.

Giddings (1995) hypothesized that complex mixtures can be described with multiple *dimensions*, such as size, shape and polarity. When multiple dimensions are present in a sample, peaks are randomly distributed in the chromatogram. Complete component separation can be achieved when the separation dimensions match the sample dimensions (provided there is sufficient resolving power in each dimension) and the resulting chromatogram will be ordered.

To illustrate the concept of matching separation dimensions to sample dimensions, consider a mixture of objects having various sizes, shapes, and gray scales, shown in Figure 5-1A. When objects are separated only by size, as in Figure 5-1B, coelutions occur among objects of different shape and gray scale. When objects are separated by two of the three sample dimensions, as in Figure 5-1C, the result is a more ordered chromatogram with less coelution. When the separation dimensions are size and gray scale, the chromatogram exhibits coelution by objects of different shape. When the separation dimensions are size and shape, the chromatogram exhibits coelution by objects of different gray scales. When objects are separated by the same three dimensions as the sample, complete separation results and the chromatogram is ordered. Ordered chromatograms are the result of matching sample and separation dimensionality and represent efficient use of peak capacity.

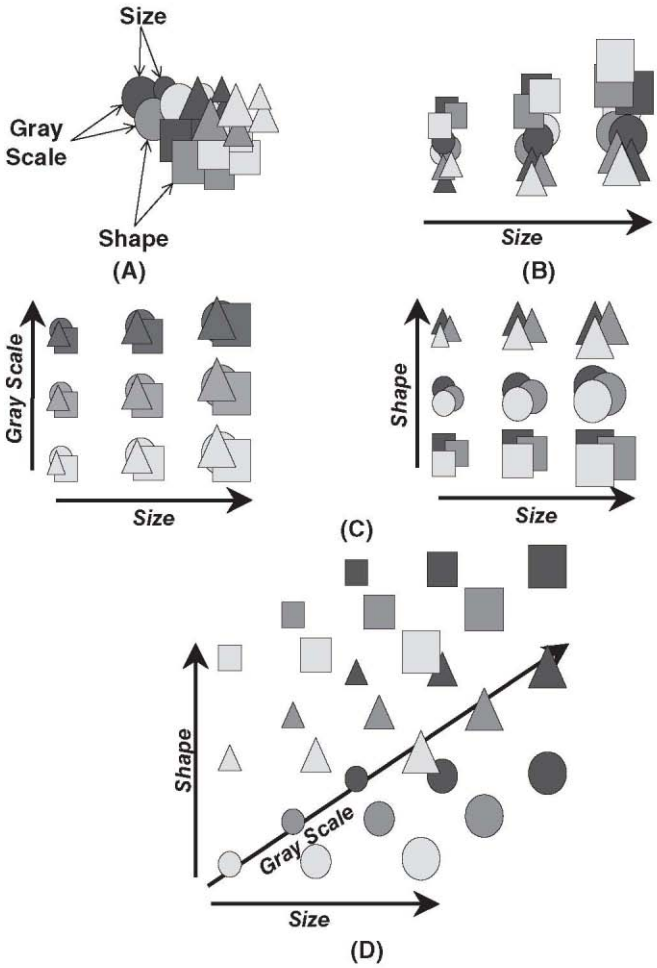

Figure 5-1 Conceptual diagram of matching mixture dimensions with separation dimensions to achieve complete separation and an ordered chromatogram. (A) Three-dimensional mixture in gray scale, shape, and size; (B) one-dimensional separation in size results in poor separation; (C) two-dimensional separation improves separation and results in a more ordered chromatogram; (D) matching mixture and separation dimensions results in complete separation and ordered chromatogram.

5.1.2 Multidimensional Methods

Until recently, multidimensional analyses of petroleum spills were accomplished primarily using gas chromatography — mass spectrometry (GC-MS) systems employing a high-resolution capillary column and a quadrapole mass spectrometer operating in either a full scan or selected-ion-monitoring mode (ASTM, 2000b). Methods such as GC-MS provide information about specific chemical classes found within oil. Although the high-resolution capillary GC column cannot resolve many of the petroleum compounds, the mass spectrometer is able to virtually separate the GC coeluents by mass because components of a specific chemical class often have unique molecular fragmentation patterns. Identification and comparison between compound classes, especially high-molecular-weight biomarkers, produce a more detailed and informative fingerprint (e.g., see Chapter 3 in this volume). GC-MS analyses have certain limitations. GC-MS methods may not always successfully differentiate similar light petroleum distillates. High-resolution GC does not have the resolving power to detect minor component differences, and the high-molecular-weight biomarkers and other compounds with unique fragmentation signatures may be absent in these products. When numerous organic compounds are not fully resolved by the GC, the

resulting full-scan mass spectra are the sum of the spectra of all coeluting compounds. This makes identification of potentially new marker compounds by library spectral matching difficult.

5.2 Comprehensive Two-Dimensional Gas Chromatography (GC × GC)

Another approach to a multidimensional separation, called comprehensive two-dimensional gas chromatography (GC × GC), has the potential to revolutionize forensic oil spill analysis. GC × GC is capable of separating an order of magnitude more compounds from complex mixtures than traditional gas chromatography (Bertsch, 2000; Phillips and Beens, 1999; Liu and Lee, 2000). GC × GC has produced chromatograms with thousands of resolved peaks from samples where traditional single-column chromatography resolved fewer than 100 peaks (Venkatramani and Phillips, 1993; Gaines et al., 1999; Frysinger and Gaines, 2001). Increased chromatographic resolution is achieved by using two chromatographic columns with different selectivity coupled together by a modulator. The modulator periodically samples the first column eluent and injects it into the second column. Figure 5-2 illustrates the concepts of comprehensive two-dimensional gas chromatography. The peak in Figure 5-2A represents a typical first-dimension chromatogram peak having a width of about 25 s. In Figure 5-2B, the modulator periodically samples the analyte mass of the first-dimension peak, compresses it, and injects it as a narrow peak into the second column. The vertical dashed lines in the figure indicate the start of each modulation cycle. Figure 5-2C shows how a fast, second-column separation can resolve coeluents present in the first dimension peak. Note that the second-dimension separation is complete before the next modulator injection. In Figure 5-2D, the detector data stream is sliced into segments and packed into a two-dimensional array. Figure 5-2E shows a contour plot created from the two-dimensional array. Peaks are positioned on a two-dimensional retention time

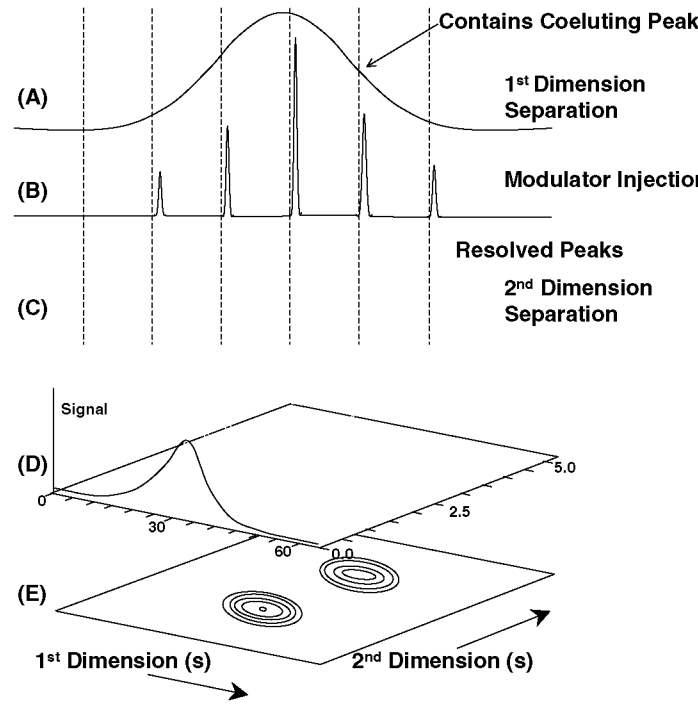

Figure 5-2 Concepts of comprehensive two-dimensional gas chromatography (GC × GC): (A) first-dimension chromatogram peak containing coeluents; (B) modulator samples first-dimension peaks and injects narrow peak into second dimension; (C) coeluents are separated in the second dimension; (D) serial flame ionization detector data stream is sliced into segments and stacked into an array; (E) array is visualized with a contour. Copyright 2002 from *GC × GC — A New Analytical Tool for Environmental Forensics*, by G.S. Frysinger et al. Reproduced by permission of Taylor & Francis Group, LLC, http://www.taylorand francis.com.

plane according to their retention time along each individual retention time axis.

GC × GC is considered *comprehensive* because all of the analyte mass from the first column is transferred to the second column. Thus, all compounds are subjected to two different separation mechanisms. GC × GC is different than two-dimensional "heart-cut" gas chromatography where one zone of analytes eluting from the first column is isolated and subsequently separated in a different column (Bertsch, 1999).

5.2.1 Modulation Techniques

The most critical component of GC × GC is the modulator. The modulator must accomplish three fundamental steps: (1) efficient trapping of the first-column eluent in a short region of the modulator capillary column; (2) rapid release and injection of the trapped compounds onto the head of the second column; and (3) rapid return to trapping conditions. Early commercial modulators employed a section of capillary containing a thick stationary phase to trap first-column eluent, and a rotating slotted heater that when swept across the trapping region, compressed the band, desorbed the trapped analytes, and injected them into the second column (Phillips et al., 1992). Many applications of GC × GC were accomplished using this modulator, including the first application of GC × GC to forensic oil spill identification (Gaines et al., 1999). Modern commercially available modulators such as the KT2004 (Zoex Corporation) employ cryogenic trapping of first-column eluent onto the modulator capillary column by use of a jet of liquid-nitrogen-cooled gas (Gorecki et al., 2004). The trapped analytes are then released into the second column by rapid heating from a dedicated hot jet. Two strategies are employed to prevent breakthrough by first-column eluents while the trap is cooling down. The first strategy employs two pairs of jets that generate two trapping locations. A special sequence of jet operation is used that alternates between the trapping locations to prevent breakthrough. A second strategy uses a loop in the modulator capillary column so that the column falls under the jets twice, thus producing two trapping locations from one cold jet, and avoids the necessity for a special sequence of jet operation. Even though only one set of jets is operating, the loop acts to delay the passage of the eluent released from the upstream trap until the downstream trap is at trapping temperature. When the trapping and releasing temperatures are properly tuned to the analytes, the modulator produces very narrow peaks on the order of 50 milliseconds for a very wide range of compounds, including those normally used to fingerprint crude oil and refined petroleum products (Gaines and Frysinger, 2004). Narrow peaks facilitate fast gas chromatographic separation on the second column necessary for the high peak capacities required to separate complex mixtures such as petroleum. Narrow peaks from spatial band compression during modulation increase signal-to-noise ratio, thus improving the detection and quantification of minor compounds (Liu and Phillips, 1994; Phillips et al., 1999; Lee et al., 2001).

Other GC × GC modulation techniques have been designed and successfully employed, some of which are in various stages of commercialization. For example, GC × GC systems have successfully used moving liquid CO_2 cryogenic modulators (Marriott and Kinghorn, 1999; Beens et al., 2001a), pulsed liquid CO_2 jet modulators (Thermo Electron Corporation) (Beens et al., 2001b), mechanical valve modulators (Bruckner et al., 1998; Seeley et al., 2000; Sinha et al., 2003; Micyus et al., 2005), and stop-flow modulators (Gorecki et al., 2004).

5.2.2 Detectors

GC × GC detectors need to have a fast response. Modulators produce very narrow injections into the second column where fast gas chromatography separates the first column coeluents. Because the chromatography on the second column is also fast, the resulting compound peaks presented to the detector remain very narrow, typically with widths at the base

of 80–400 milliseconds depending on the second column retention. To properly sample the narrowest peaks requires a data rate of at least 100 Hz, but a slower data rate of 50 Hz can be used for the wider peaks. Flame ionization detectors are most widely used, but element-specific detectors such as nitrogen chemiluminescence (Wang et al., 2004), sulfur chemiluminescence (Blomberg et al., 2004), and atomic emission (van Stee et al., 2003) show promise to analyze petroleum with possible applications to oil spill fingerprinting.

When a GC × GC is coupled to a mass spectrometer, an additional dimension of information about the sample is available and can be used to identify components separated from the complex mixture. The mass spectrometer can also be used as an additional separation mechanism resulting in a three-dimensional separation. Quadrupole mass spectrometers operating in full scan mode are too slow to properly sample a GC × GC peak unless that peak is broadened (Frysinger and Gaines, 1999). Fast time-of-flight mass spectrometers (TOFMS) that operate with spectral acquisition rates of 100–200 Hz are well-suited for GC × GC and have been used for numerous studies (Dalluge et al., 2003). A GC × GC-TOFMS system is commercially available (LECO Corporation).

5.2.3 Data Processing

GC × GC presents information technology challenges in data handling, visualization, processing, analysis, and reporting due to the quantity and complexity of GC × GC data (Reichenbach et al., 2004). During the early stages of GC × GC development, analysis of GC × GC chromatograms was accomplished by visual means, and peaks were integrated manually. Commercially available software such as Transform (Fortner Software LLC) and Matlab (The Math Works, Inc.) produces interpolated color contour plots from the two-dimensional retention time array. Data are interpolated between contours according to a predefined color palette. The detailed visual nature of the GC × GC plots facilitates effective comparisons between chromatograms. Target peaks are integrated by summing the array data that comprise that peak. This manual integration was made easier due to the improved separation by GC × GC of a target peak from the rest of the sample. This manual approach, while especially useful for visual comparison-based applications such as petroleum fingerprinting, is extremely cumbersome and time-consuming.

Fortunately, new software tools have become available to more easily extract useful information from GC × GC data. GC Image (GCImage LLC) is a software system developed at the University of Nebraska-Lincoln (Reichenbach et al., 2004) that uses advanced information technologies to process and visualize GC × GC data, detect peaks, compare chromatograms, and perform peak deconvolution, pattern recognition and other data mining tasks. ChromaTOF (Leco Corporation) is another software program designed to control Leco's commercially available GC × GC-TOFMS system that has similar functions. Both GCImage and ChromaTOF make effective use of the tremendous amount of data generated when a time-of-flight mass spectrometer is used as a GC × GC detector, including spectral library matching and extracted ion chromatograms. HyperChrom (Thermo Electron Corporation) is a third software program designed to control Thermo Electron's commercially available GC × GC system with flame ionization detection and employs various data processing and visualization capabilities.

GC × GC and GC × GC-TOFMS data structure is well-suited for multivariate quantitative analysis, deconvolution, and pattern matching. New advanced numerical approaches to data mining include chemometric signal deconvolution (Sinha et al., 2004), reduced peak pattern variations that improved template matching (Ni et al., 2005), and enhanced limits of detection using bilinear chemometric analysis (Fraga et al., 2000). Advanced statistical methods will have direct impact on applications such as petroleum fingerprinting by

improving current fingerprinting methods and identifying new target compounds useful to fingerprint samples that are not amenable to current methods because they do not contain the appropriate target compounds. For example, analysis of variance (ANOVA)-based feature selection was effectively used to determine chromatogram features important to the pattern recognition of jet fuels (Johnson and Synovec, 2002).

5.2.4 GC × GC Chromatogram

Figure 5-3 shows a chromatographic separation of *Exxon Valdez* cargo oil. Figure 5-3A is a one-dimensional separation using a nonpolar 100% polydimethylsiloxane stationary phase. The carbon range shown is from about C_8 to C_{47} [in part obscured due to (C) inset]. The presence of a hump of unresolved compounds means few compounds have been separated from the mixture. Figure 5-3B is a GC × GC two-dimensional separation visualized as an interpolated color contour. The first dimension separation along the *x*-axis is on a nonpolar 100% polydimethylsiloxane stationary phase and under the same chromatographic conditions as Figure 5-3A. The second dimension separation along the *y*-axis is on a polar 50% phenyl polysilphenylene stationary phase. The polarity separation in the second dimension resolved many compounds that coeluted after the first dimension. Compounds that are fully resolved from the mixture are seen as individual spots or peaks on the two-dimensional retention time plane. The back-

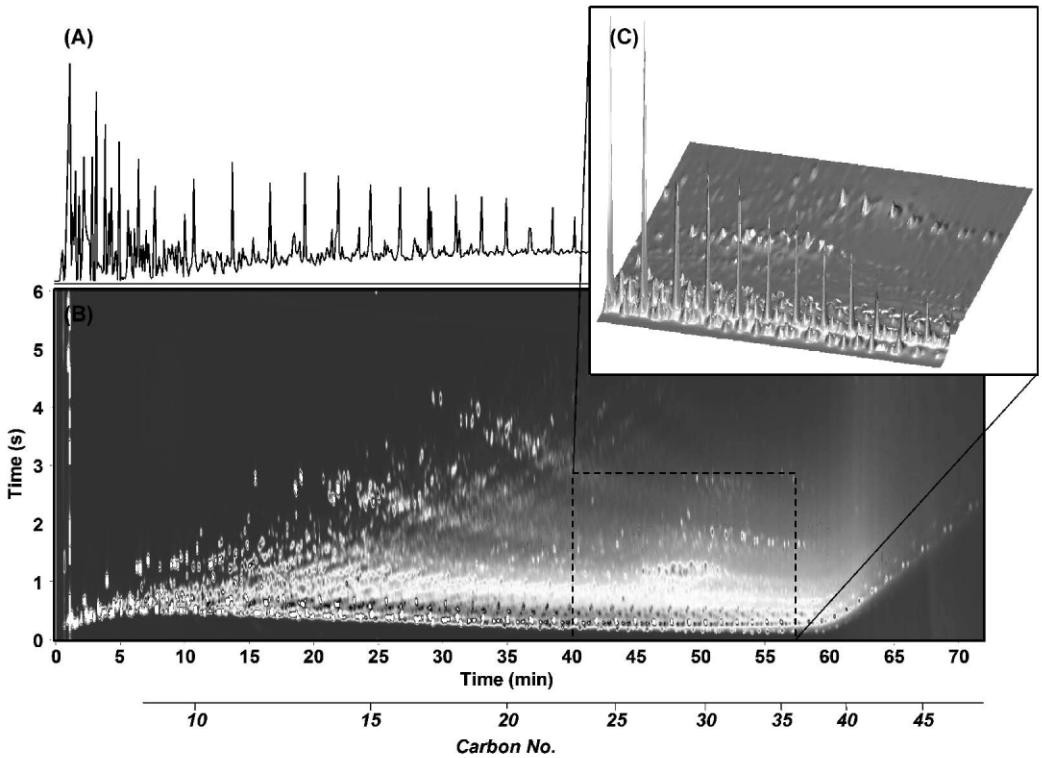

Figure 5-3 Chromatograms of *Exxon Valdez* cargo oil: (A) One-dimensional gas chromatogram using a nonpolar 100% polydimethylsiloxane stationary phase; (B) GC × GC volatility-by-polarity interpolated color contour plot. The first dimension is a separation using a nonpolar 100% polydimethylsiloxane stationary phase and the second dimension is a separation using a polar 50% phenyl polysilphenylene stationary phase; (C) a small portion of the GC × GC chromatogram visualized as a mountain plot. The mountain plot is excellent for visualizing relative differences among neighboring peaks. See color plate.

ground signal is light blue. Peak abundance is colored from white (low) to red (medium) to dark blue (high). To view the low abundance peaks, the highest peaks have been chopped off and this appears as a white portion in the center of the peak.

The crude oil chromatogram has hundreds of resolved peaks, but given the tremendous chemical complexity of the sample, two dimensions of separation are not sufficient to resolve all compounds. This is seen by the many peaks at the bottom of Figure 5-3B that are not fully resolved. It is also possible that some of the individual peaks in the upper portion of the chromatogram have coeluents remaining after the two-dimensional separation as well. Figure 5-3C is a small portion of the GC × GC chromatogram in Figure 5-3B visualized as a mountain plot. Mountain range plots use color and peak height to visualize signal size. Mountain range plots are especially good at revealing small peaks among neighboring larger peaks in GC × GC chromatograms of samples with a wide range of constituent concentrations.

5.2.5 Peak Identity and Chromatogram Structure

Several methods are used to identify the resolved peaks in the GC × GC chromatogram. First, a peak can be identified with a chemical standard. In GC × GC, a match in both the first- and second-dimension retention times provides compound identity with a greater degree of certainty than one-dimensional gas chromatography using a single retention time. A second method to identify peaks in a GC × GC chromatogram is by direct comparison between GC-MS and GC × GC data. A direct comparison is possible if the chromatography columns, conditions, and first-dimension retention times are matched (Frysinger and Gaines, 2001). Figure 5-4 shows a portion of a volatility-by-polarity GC × GC chromatogram of an *Exxon Valdez* cargo oil sample, along with GC-MS extracted ion chromatograms for ions that are diagnostic for sterane, hopanes, and triaromatic sterane biomarker groups. There is excellent retention time and abundance correlation between the GC × GC and GC-MS extracted ion chromatogram peaks. The excellent correlation allows the chemical identities of the extracted ion chromatogram peaks to be transferred to the GC × GC chromatogram band. A third method to identify peaks in the GC × GC chromatogram is to use a mass spectrometer interfaced directly with the GC × GC instrument. Since GC × GC greatly improves the separation of peaks in complex mixtures, a pure compound peak is presented to the mass spectrometer. For example, five GC × GC-MS spectra with corresponding chemical structures are shown in Figures 5-5D to 5-5 H. The mass spectrum of each compound is very clean and is not affected by other compounds that would otherwise coelute and interfere in a GC-MS analysis. The GC × GC-MS spectrum for naphthalene in Figure 5-5D does not have the extraneous ions that degrade the GC-MS spectrum in Figure 5-5A. The GC × GC-MS spectrum for 1,2,3-trimethylbenzene in Figure 5-5E shows how GC × GC-MS can isolate and measure the spectrum for just one of the components contributing to the complex GC-MS spectrum in Figure 5-5B. GC × GC-MS analysis also improves the detection of low-abundance molecular ion peaks. The *m/z* 156 molecular ion peak for 4-methyldecane and the *m/z* 140 molecular ion for *n*-butylcyclohexane are observed in Figure 5-5F and Figure 5-5G, respectively. In a normal GC-MS analysis, these small molecular ion peaks would most likely be lost in the baseline noise. The advantage of GC × GC-MS is that the resulting pure-component spectra can be accurately interpreted and compared to standard mass spectral libraries to determine the chemical identity. Hence, GC × GC-MS analysis can simultaneously provide both the selectivity provided by GC-MS selected ion monitoring and the compound identification provided by a GC-MS full-scan analysis.

A fourth method of peak identification makes use of the ordered chromatograms found in volatility-by-polarity GC × GC separations. This order provides valuable insights

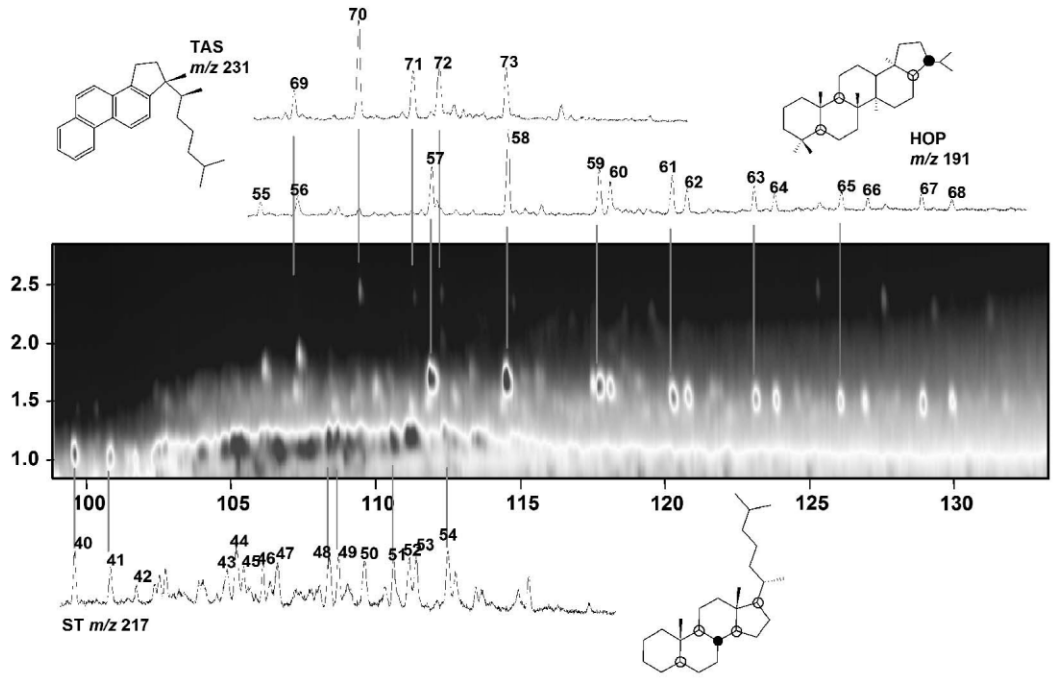

Figure 5-4 A small portion of a volatility-by-polarity GC × GC chromatogram of *Exxon Valdez* cargo oil showing the region containing the triaromatic sterane, hopanes, and sterane biomarkers. GC-MS extracted ion chromatograms (EICs) of these biomarker target ions are overlaid for identification and comparison. Peaks numbered on each EIC are identified in Frysinger and Gaines (2001). The structures of 5α,14α,17α(H)-cholestane (20R) (peak 46), 17α,21β(H)-hopane (peak 58) and cholestane (20S) (peak 69) are included for reference. *x*-axis: minutes; *y*-axis: seconds. Reproduced with permission from Frysinger and Gaines (2001). Copyright 2001 Wiley-VCH.

into the properties of unknown species and allows for easy identification of homologous series of compounds within complex mixtures. In Figure 5-5, the first dimension volatility-based separation sorts the complex mixture by boiling point. Since the first dimension is temperature programmed, the homologous series of *n*-alkanes is regularly spaced across the bottom of the two-dimensional retention time plane. The second-dimension separation sorts the complex mixture by functional group from least polar at the bottom to most polar at the top. At the bottom of the GC × GC chromatogram are the nonpolar *n*-alkanes and branched alkanes. Immediately above the alkanes are the one-ring and two-ring cycloalkanes. Above the cycloalkanes are the one-ring and two-ring aromatics. The location of a specific compound in the two-dimensional volatility-by-polarity plane depends primarily on the number of total carbons and the extent to which the chemical structure contributes to molecular polarity.

An important consequence of the first- and second-dimension ordering is that structural isomers are grouped into linear bands. For example, one prominent band in Figure 5-5 is the three-carbon substituted alkylbenzene isomers, which is identified as Figure 5-5C by comparison with the *m/z* 120 extracted ion chromatogram. The structural isomers cover a range of volatility because the boiling points of the isopropyl- and propylbenzene are lower than the ethylmethyl- and trimethylbenzene isomers, but they all have very similar polarity due to the influence of the benzene ring. The last two peaks in the band are indan [peak (I)] and indene [peak (J)], which do not

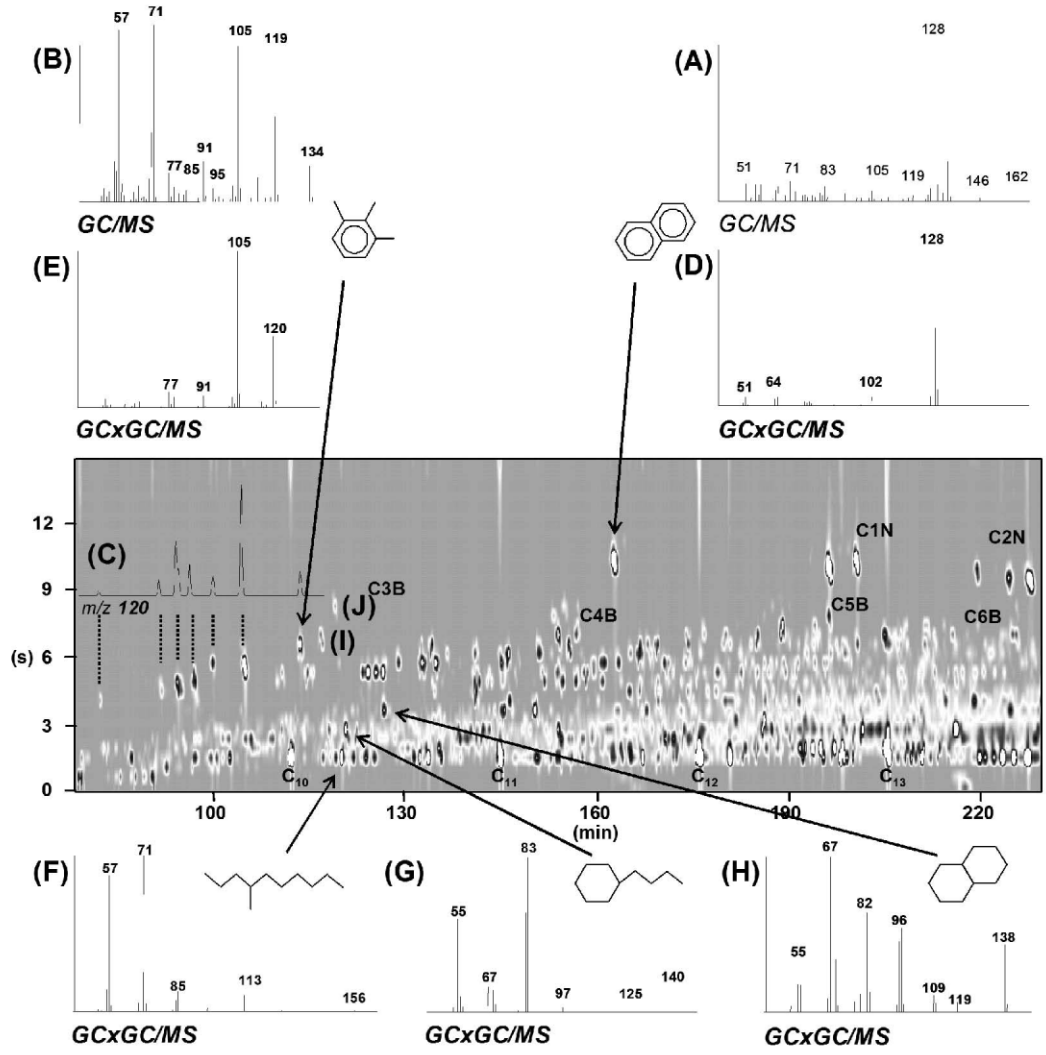

Figure 5-5 Partial GC × GC-MS chromatogram of diesel fuel. The *x*-axis is a volatility-based chromatographic separation on a 100% polydimethylsiloxane stationary phase. The *n*-alkanes decane (C_{10}) to tridecane (C_{13}) are identified. The *y*-axis produces polarity-based chromatographic separation on a 14% cyanopropylphenyl methylsiloxane stationary phase. The MS total ion intensity data are displayed as an interpolated color contour. Overlay data: (A–B) GC-MS spectra for specific retention times; (C) GC-MS *m/z* 120 extracted ion chromatogram; (D–H) GC × GC-MS spectra and structures of naphthalene, 1,2,3-trimenthylbenzene, 4-methyldecane, *n*-butylcyclohexane, and decahydronaphthalene, respectively; (I) indan; (J) indene. Copyright 2002 from *GC × GC — A New Analytical Tool for Environmental Forensics*, by G.S. Frysinger et al. Reproduced by permission of Taylor & Francis Group, LLC, http://www.taylorandfrancis.com.

have a corresponding peak in the *m/z* 120 extracted ion chromatogram. Indan and indene peaks would be found in the *m/z* 118 and *m/z* 116 extracted ion chromatograms, respectively. Indan has a cyclopentane ring attached to the benzene, and indene has a cyclopentene ring. In GC × GC, it is logical to extend the family of three-carbon substituted alkylbenzene isomers to include indan and indene because even though their molar masses are different, they both have three carbons attached to the benzene ring in some

manner. Most importantly, their volatility and polarity properties place them at the end of that band.

The two-dimensional order also produces other bands in the GC × GC chromatogram. For example, the four-carbon (C4B), five-carbon (C5B), and six-carbon substituted alkylbenzenes (C6B) each form bands to the right of the three-carbon substituted alkylbenzenes (C3B; Figure 5-5). At greater second-dimension retention, the one-carbon naphthalene (C1N) and part of the two-carbon naphthalene (C2N) bands are ordered to the right of the naphthalene peak. The retention time separation between successive bands is about the same as the separation between members of the *n*-alkane homologous series.

The use of ordered bands to help identify peaks can be facilitated by optimizing the two-dimensional chromatography. In Figure 5-5, the nonpolar alkanes found at the bottom of the volatility-by-polarity GC × GC chromatogram are not very well separated into isomer bands because their polarity difference is very small so their retention time on the second column is the same. Better separation can be achieved using a different second column stationary phase. For example, Figure 5-6(A) shows a portion of a volatility-by-polarity GC × GC separation of the saturates fraction of a sediment sample containing biodegraded petroleum (Frysinger et al., 2003). The line of peaks across the bottom of the chromatogram represents the branched alkanes. The isoprenoid biomarkers norpristane, pristane, and phytane are labeled. The peaks above the branched alkanes are the cycloalkanes, with the position of *n*-octylcyclohexane shown. Other peaks at about the same second-dimension retention are alkylcyclohexane or alkylcyclopentane isomers. Peaks at greater second-dimension retention are multi-ring cycloalkanes.

The branched alkanes and cycloalkanes in Figure 5-6(A) are not ordered into distinct sloping bands with carbon number spacing. This suggests that the selectivity of the GC × GC separation is not properly tuned to the dimensionality of the mixture. In addition, there is a lot of unused peak capacity (open space) in the two-dimensional retention time plane. A "shape" selective column was better able to separate the branched alkanes and cycloalkanes from one another. Figure 5-6B shows the resulting volatility-by-shape GC × GC chromatogram that contains many separated peaks organized into numerous groups that are spread across the entire second dimension of the GC × GC chromatogram. The branched alkanes, poorly resolved in the GC × GC separation shown in Figure 5-6A, are now separated and organized into numerous diagonal bands (Figure 5-6B). The different bands arise from different alkane substitution patterns. For example, all monomethyl substituted alkanes form one band, and all dimethyl alkanes may form the adjacent band. Circles on the chromatogram indicate the two-dimensional retention time positions of the *n*-alkanes (*n*-C_{13} through *n*-C_{20}). Due to microbial degradation of the sample, only trace peaks remain at each *n*-alkane position. The number of resolved cycloalkane compounds is also significantly increased in this sample. The cycloalkane compounds are now grouped into bands and spread across the full two-dimensional retention time plane of the gas chromatogram. A small region in Figure 5-6B is expanded in Figure 5-6C to show branched alkane band detail.

Figure 5-7 is a volatility-by-polarity GC × GC chromatogram of a crude oil showing the location of various classes of petroleum constituents that are important to fingerprinting petroleum products. The crude oil spans the carbon number range from about C_8 to C_{47}. A volatility-by-polarity separation of crude oil produces chemical class separation of *n*-alkanes, branched alkanes, cycloalkanes, and one- and multiring aromatics. Individual chemical classes exhibit banding similar to that shown in Inset A of Figure 5-7. Isomers of alkyl-substituted naphthalenes are grouped into bands of the same total carbons. Bands increase in total carbons going from left to right. Biphenyl is located near the C2-naphthalene band because it has 12 total carbons. Because biphenyl has a slightly different polarity than C2-naphthalene, it is

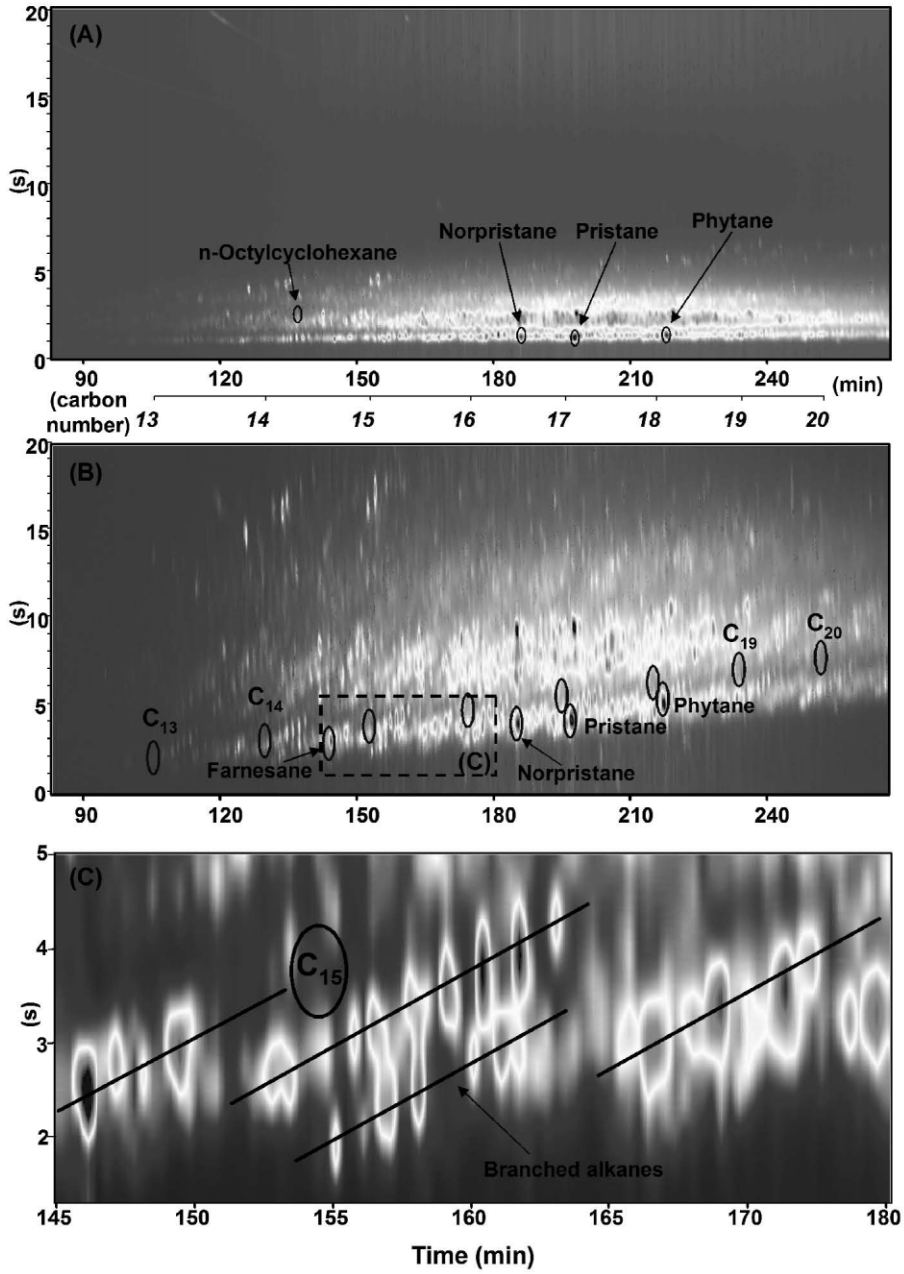

Figure 5-6 Effect of changing the second-dimension stationary phase on the separation of nonpolar saturates: (A) GC × GC chromatogram of the saturates fraction of a sediment extract using a polar second-dimension 14% cyanopropylphenyl polysiloxane stationary phase; (B) GC × GC chromatogram of the same saturates fraction using a chiral γ-cyclodextrin second-dimension stationary phase. The expected positions of the *n*-C_{13} to *n*-C_{20} alkanes are marked with circles. The region inside the dotted lines is expanded in (C); (C) expanded region showing expected position of *n*-C_{15} and location of branched alkane bands. Reprinted with permission from Frysinger et al., 2003. Copyright 2003, American Chemical Society. See color plate.

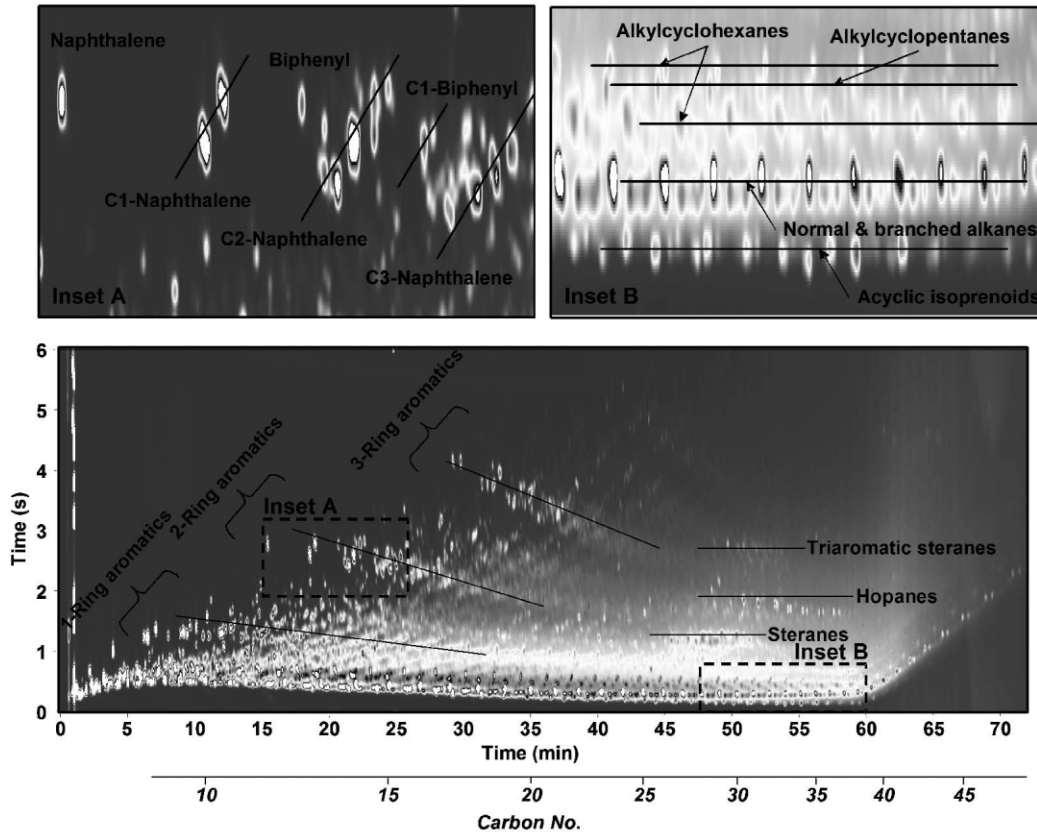

Figure 5-7 Location of petroleum chemical classes on a volatility-by-polarity GC × GC chromatogram. Nonpolar alkanes are located at the bottom, with one- and multiring aromatics further up the *y*-axis as their polarity increases. Inset A: naphthalene region showing bands of alkyl-substituted naphthalenes and biphenyls; Inset B: nonpolar region showing high-resolution separations of higher boiling (C_{28}+) acyclic isoprenoids, normal and branched alkanes, and cyclic alkanes. See color plate.

separated from the C2-naphthalene band. C1-biphenyl has a slightly different polarity than C3-naphthalene, so it is also separated from the C3-naphthalene band. The distance between biphenyl and C1-biphenyl is the same as the distance between the C1- and C2-naphthalene bands. Inset B of Figure 5-7 shows the detailed separation of the higher boiling (C_{28}+) acyclic isoprenoids, normal and branched chain alkanes, and cyclic alkanes achievable with GC × GC. The high-resolution separation of nonpolar and higher boiling compounds makes it possible to investigate new classes of weathering resistant petroleum marker compounds potentially useful for fingerprinting.

5.2.6 GC × GC Petroleum Applications

From the early stages of GC × GC development, petroleum analysis and characterization were logical areas for application. Petroleum samples contain thousands of compounds that are a real challenge to separate by typical one-dimensional chromatographic methods. GC × GC provides the requisite separation power to separate major and minor individual compounds as well as major and minor compound chemical groups (e.g., PIONA: paraffins, isoparaffins, olefins, naphthenes aromatics) from the complex petroleum matrix. For example, group-type analysis has

been done for heavy naphtha (Vendeuvre et al., 2005b), naphtha, and other petrochemicals (Vendeuvre et al., 2004; Prazen et al., 2001; Schoenmakers et al., 2000; Blomberg et al., 1997), diesel fuel (Vendeuvre et al., 2005a; Gaines et al., 1999), kerosene (van Deursen et al., 2000), and gasoline (Frysinger and Gaines, 1999). Target compound separation and analysis has been done for biomarkers in crude oil (Frysinger and Gaines, 2001), hydrocarbons (Gaines et al., 1999), nitrogen compounds (Wang et al., 2004), and sulfur compounds (Blomberg et al., 2004) all in diesel fuel, and arson accelerant marker compounds in petrochemicals (Frysinger and Gaines, 2002). This partial list of GC × GC petroleum applications illustrates the enormous potential for GC × GC as a forensic oil spill technique. GC × GC provides a very high-resolution separation with a data output amenable to visual and quantitative comparison between samples using both individual compounds and classes of compounds. Furthermore, GC × GC separations elucidate chemical structure, and therefore new potential target compounds, not usually seen from traditional gas chromatographic separations of petroleum samples.

5.3 Applications of GC × GC to Fingerprint Oil Spills

5.3.1 Mobile Bay Marine Diesel Fuel Spill

The first application of GC × GC to oil spill fingerprinting involved a spill of approximately 100 gallons of marine diesel fuel into a bay near Mobile, Alabama, USA (Gaines et al., 1999). In this example, GC × GC was used to determine qualitative and quantitative similarities and differences between the spill and suspected source samples. The high resolving power of GC × GC separated many hundreds of compounds from the petroleum matrix, making it possible to select individual compounds or groups of compounds for analysis. For this oil spill analysis, several traditional marker classes were used including alkanes, alkylbenzenes, alkylnaphthalenes, and phenanthrenes. One nontraditional class of petroleum constituents found useful was the alkylcyclohexanes. The overall results compared favorably with standard GC fingerprinting methods.

A slightly weathered spill sample (designated Spill) was taken from the surface of the water approximately 24 hr after the spill. Two potential source samples (designated Source 1 and Source 2) were collected from the fuel tanks of two nearby suspect fishing vessels.

Figure 5-8 shows a portion of the volatility-by-polarity chromatogram from each of the three samples analyzed by GC × GC. The spill sample is shown in panel A, one potential source, Source 1, is shown in panel B and one potential source, Source 2, is shown in panel C. The *n*-alkane range is approximately tridecane (C_{13}) through eicosane (C_{20}). This region contained features that were suitable for fingerprinting of middle distillate fuels. Earlier eluting compounds were not suitable for fingerprinting because of losses due to weathering by evaporation and dissolution while the spilled oil was on the water.

Each sample was compared to the spill qualitatively by visual comparison and quantitatively by integration of selected peaks and bands of peaks. Visual similarities and differences between the spill and source chromatograms were made by comparing the presence or absence of peaks at a particular location on the retention time plane and their relative size. Each source sample exhibits a high degree of similarity with the spill sample. The alkane peaks, found in a line along the bottom of the chromatograms, are very similar, as is the distribution of alkyl-substituted benzene, naphthalene, and phenanthrene compounds found in the aromatic region beginning just above the alkanes (see Figure 5-7 for additional peak locations). The numerous similarities are due to the facts that all three samples are marine diesel fuel and that it is likely the suspect sources fueled from the same fuel source.

Although both suspect source samples are very similar to the spill sample, there are

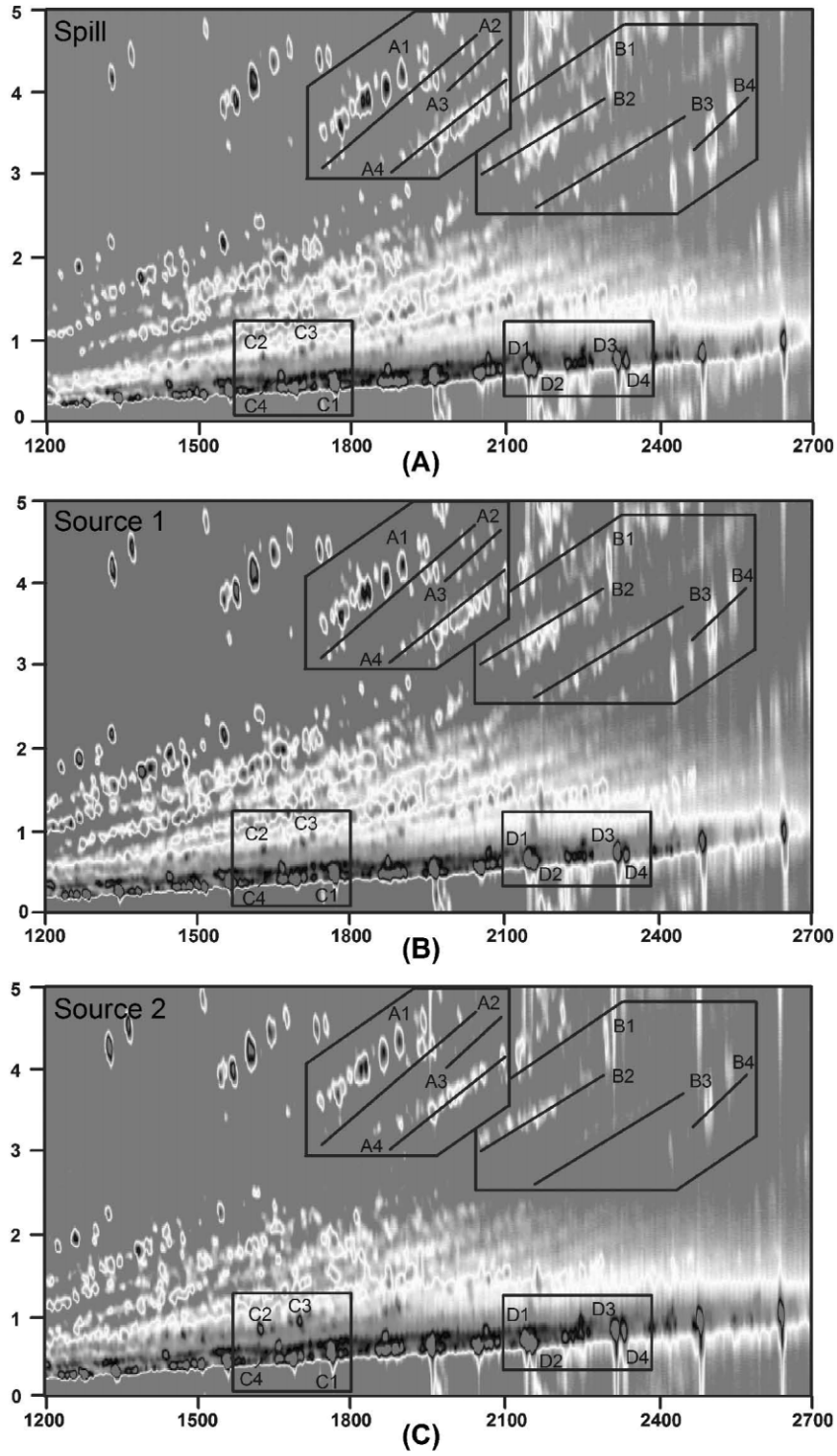

Figure 5-8 Portion of a volatility-by-polarity GC × GC-FID chromatogram from each of the three samples compared: (a) spill; (b) and (c) potential spill sources. Both axes are in seconds. The boxes contain chemical families and individual compounds used to qualitatively and quantitatively compare two potential source samples with the spill samples. The first column separation shown along the *x*-axis was accomplished with a nonpolar 5% phenylmethylsiloxane stationary phase. The second column separation shown along the *y*-axis was accomplished with a polar polyethylene glycol/siloxane copolymer stationary phase. Reprinted with permission from Gaines et al., 1999. Copyright 1999, American Chemical Society. See color plate.

numerous small differences that are easily visible in the chromatograms. For example, Source 2 exhibits noticeably fewer peaks in the heavy aromatic region (upper right corner of the chromatograms) than the Spill. Several of these minor chromatogram differences were selected for quantitation. Each chromatogram in Figure 5-8 shows four windows that identify the regions used to quantify differences. Within each window, selected peaks and bands of peaks were integrated and normalized to a specific peak located inside the same window.

Window A contains naphthalene compounds known to be prevalent in petroleum products, are resistant to evaporative weathering, and are useful for fingerprinting. Band A4 contains four carbon substituted naphthalenes (C4N), while bands A2 and A3 contain unidentified compounds of similar volatility and polarity to the alkylnaphthalenes. These bands were normalized to A1, which is 2,3,5-trimethylnaphthalene. The integration results are shown in Figure 5-9(A). The data labeled "quality control" (QC) is a repetitive analysis of the spill sample. The uncertainty in the integration result is 10% (Gaines, 1998) and shown as an error bar on the graph. The bar graph indicates that Source 1 and Spill are similar, while Source 2 and the Spill are different.

Window B in Figure 5-8 contains naphthalene and phenanthrene compounds. The B2 band contains five-carbon-substituted naphthalenes (C5N) and the B3 band contains six-carbon-substituted naphthalenes (C6N). The B4 band contains one-carbon-substituted

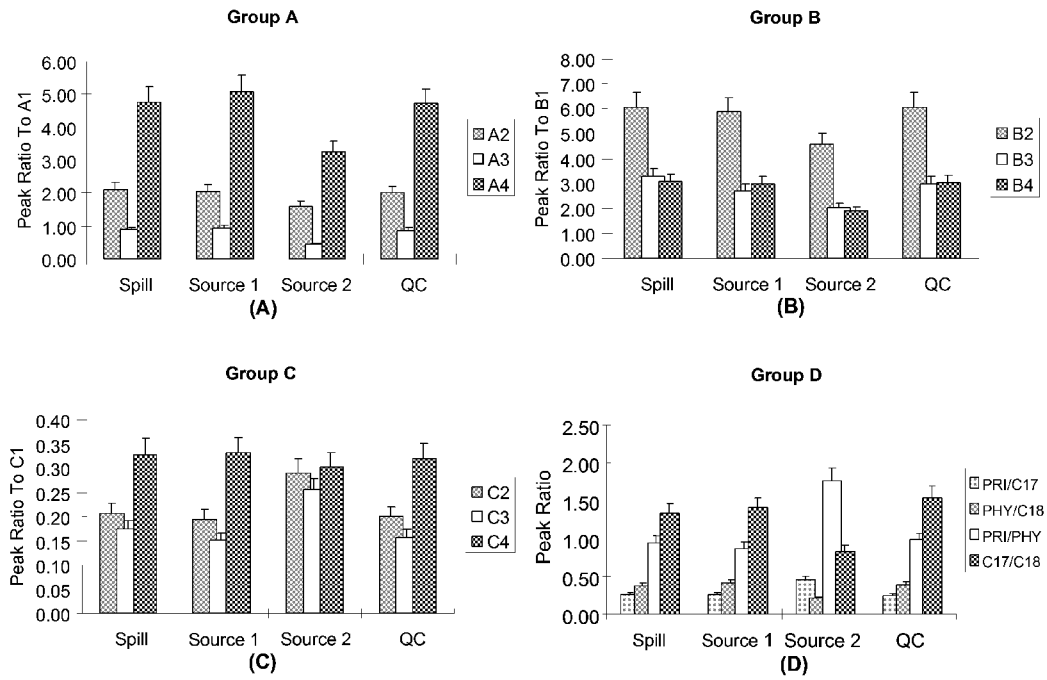

Figure 5-9 Quantitative comparisons between spill sample and two potential source samples from Figure 5-8. A quality-control (QC) sample, split from the spill, was also quantified. Each panel represents the results of integrating peaks within an individual box shown in Figure 5-8. Each bar represents the total peak or band of peaks integration results normalized to the first peak in the box. The error bar represents an estimated 10% variation calculated from replicate data, but is shown only in the plus direction. Compound classes represented: (a) alkylnaphthalene bands normalized to 2,3,5-trimethylnaphthalene; (b) alkylphenanthrenes normalized to phenanthrene; (c) cycloalkanes normalized to pentadecane; (d) heptadecane, octadecane, pristine, and phytane normalized to each other. Reprinted with permission from Gaines et al., 1999. Copyright 1999, American Chemical Society.

phenanthrenes. The bands are integrated and normalized to B1, identified as phenanthrene, and shown in Figure 5-9B. The bar graph indicates that Source 1 and Spill are similar, while Source 2 and the Spill are different.

Window C in Figure 5-8 contains alkane and cycloalkane compounds. The latter of these groups are rarely used in traditional fingerprinting methods, but the differences observed in the GC × GC separation suggest they may be useful in discriminating between similar samples. The peak C1 is *n*-pentadecane (*n*-C_{15}), C2 and C3 are tentatively identified by mass spectral library search as two isomers of pentmethyldecahydronaphthalene, and C4 is *n*-octylcyclohexane. The integration results of peaks C2-C4 are normalized to C1 and shown in Figure 5-9(C).

Window D in Figure 5-8 contains two widely used marker compounds. D2 is pristine and D4 is phytane. D1 is *n*-heptadecane (*n*-C_{17}) and D3 is *n*-octadecane (*n*-C_{18}). Scientists use four different ratio combinations to discriminate between samples, and these are shown in Figure 5-9(D). The bar graph indicates that Source 1 and Spill are similar, while Source 2 and the Spill are different.

On the basis of both qualitative and quantitative results (Figures 5-8 and 5-9, respectively), Source 1 was determined to be a probable match with the Spill. These results are consistent with the conclusions of the USCG MSL who employed high-resolution gas chromatography (ASTM, 2000a) and GC-MS (ASTM 2000b) standard methods of analyses to determine the source of the spill.

5.3.2 West Falmouth No. 2 Fuel Oil Spill

In this application, GC × GC identified compositional changes in the unresolved complex mixture (UCM) of a No. 2 fuel oil found in sediments some 30 years after being spilled (Reddy et al., 2002). Many chemical classes within the UCM were found to be remarkably persistent including branched alkanes, acyclic isoprenoids, cyclic alkanes, and polynuclear aromatic hydrocarbons (PAHs).

On September 16, 1969, the barge *Florida* went aground near West Falmouth, Mass., and spilled between 650,000 and 700,000 liters of No. 2 fuel oil into Buzzards Bay (Figure 5-10). Strong southwesterly winds mixed the oil into the water column and drove it toward Wild Harbor, located about 1 km north of the spill. Despite the use of oil booms, both subtidal and intertidal areas of Wild Harbor were heavily contaminated with oil. Oil entered the tidal Wild Harbor River, deposited in quiet marsh areas, and sorbed to sediments and grasses at the edge of the river.

The close proximity of Wild Harbor to the Woods Hole Oceanographic Institution made the contaminated area very convenient for the study of long-term fate and effects of petroleum hydrocarbons in the environment, and numerous studies were conducted (Reddy et al., 2002 and refs. therein). One site heavily studied was site M-1, shown in Figure 5-10. Sediment samples analyzed by conventional GC periodically after the spill event showed first a loss of oil compounds in the *n*-C_{10} to *n*-C_{13} alkane range due to evaporation and/or water-washing, and then progressive loss of the chromatographically resolved *n*-alkane peaks by preferential microbial degradation. By 1973, only a baseline hump comprised of an unresolved petroleum compound remained (Reddy et al., 2002).

Marsh sediments collected at the M-1 site in 1989, 20 years after the spill, confirmed the presence of oil residues in Wild Harbor sediments (Teal et al., 1992). In the Teal study, conventional gas chromatograms showed a UCM of petroleum compounds similar to those observed in 1973. Gas chromatography-mass spectrometry analysis showed elevated levels of PAHs in the sediments. The persistence of oil at this site after 20 years was attributed to the heavy contamination of the area by the spill, the high organic carbon content and anoxic conditions in the marsh sediments that hindered microbial degradation, and the presence of a low-energy environment that reduced flushing and water-washing. In particular, the anoxic conditions in the sediment apparently permitted little or no anaerobic degradation of the petroleum.

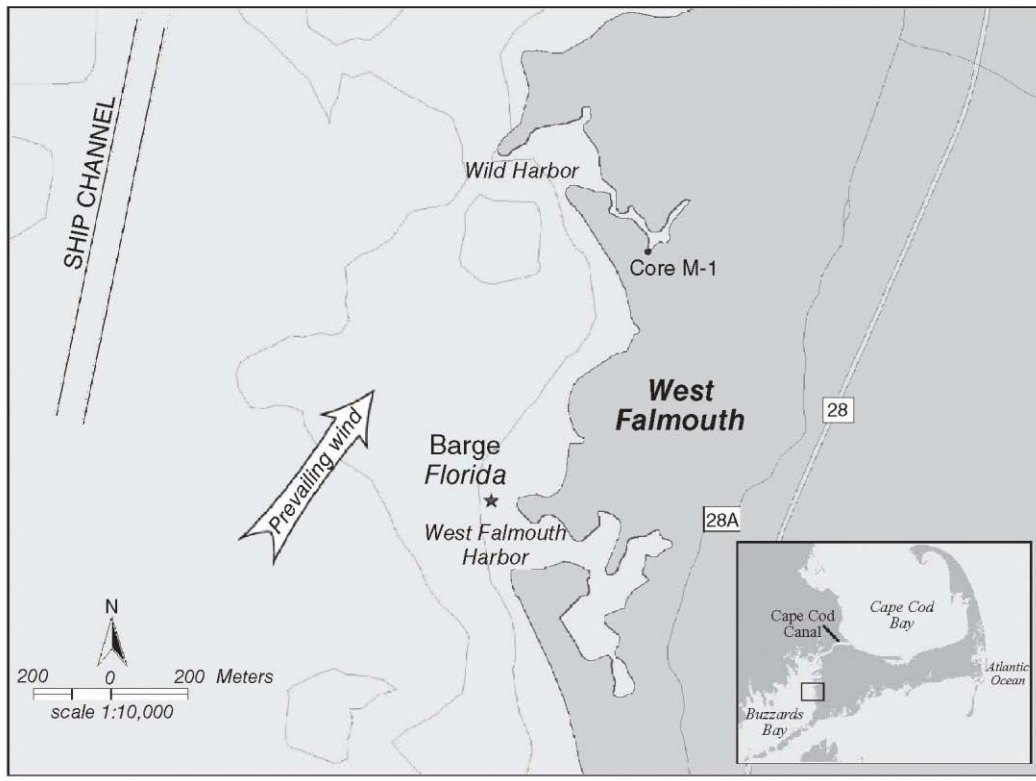

Figure 5-10 Map of the general area near the 1969 grounding of the barge *Florida*.

In 2000, conventional GC of the sediment extract shows little change in the petroleum composition over nearly 30 years since the spill. Figure 5-11 shows a comparison between conventional GC-FID chromatograms of the 1973 and 2000 sediment extracts. The two chromatograms were aligned according to *n*-alkane retention index and exhibit a UCM hump characteristic of degraded petroleum. Unfortunately, these one-dimensional chromatograms provide little information about the chemical composition of the UCM. GC × GC is better suited for analyzing the UCM because of increased resolution and the grouping of compounds by chemical class into bands.

Figure 5-12 shows the one-dimensional gas chromatogram and volatility-by-polarity GC × GC chromatogram of the sediment extract taken at the site in 2000. The GC × GC separation was able to resolve hundreds of

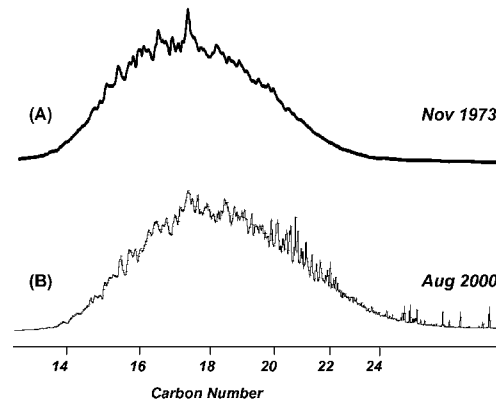

Figure 5-11 Gas chromatograms of Wild Harbor marsh sediment extracts: (A) Nov. 1973; (B) Aug. 2000. Reprinted with permission from Reddy et al., 2002. Copyright 2002, American Chemical Society.

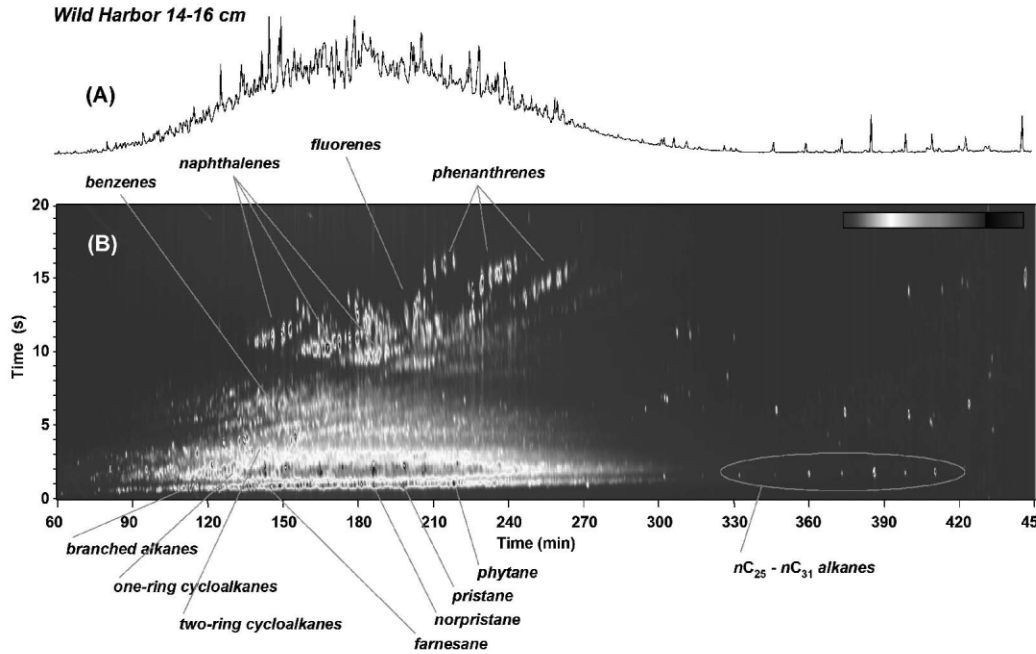

Figure 5-12 Chromatograms of a Wild Harbor sediment extract, Aug. 2000: (A) Conventional one-dimensional gas chromatogram. The separation was accomplished using a nonpolar polydimethylsiloxane stationary phase; (B) volatility-by-polarity GC × GC chromatogram. The first column separation along the *x*-axis was accomplished using a nonpolar polydimethylsiloxane stationary phase. The second column separation was accomplished using a polar 14%-cyanopropylphenyl polysiloxane stationary phase. Reprinted with permission from Reddy et al., 2002. Copyright 2002, American Chemical Society. See color plate.

compounds from the UCM, and analysis of the GC × GC chromatogram reveals several interesting features. The *n*-alkane band normally found in GC × GC chromatograms of unweathered No. 2 fuel oil is no longer present. However, at long retention times, the biogenic (derived from plant wax) *n*-C_{26}–*n*-C_{33} alkanes are present. Despite the loss of the *n*-alkanes, nearly all other compound classes appear to persist in the sediment extract. For example, numerous branched alkanes, including acyclic isoprenoids farnesane, norpristane, pristine, and phytane, are evident in the GC × GC chromatogram. This finding is contrary to studies by Burns and Teal suggesting that branched alkanes at this site were completely degraded within the first seven years after the spill (Burns and Teal, 1979) because they could no longer chromatographically resolve phytane from the UCM background. GC × GC resolved phytane from the background and showed the phytane-to-background ratio was unchanged from the mid-1970s. GC × GC also showed that the UCM contains potentially valuable forensic information conventional GC cannot distinguish from the background.

Because of the susceptibility of the *n*-alkanes to microbial degradation, Volkman et al. (1984) developed a nine-point scale that spans from one (no biodegradation) to nine (extreme biodegradation) that was later applied to refined petroleum products (Burns et al., 2000). (Also see Chapter 11 herein.) The West Falmouth sediments would be ranked between three and four because *n*-alkanes have been removed but alkylcyclohexanes and alkylbenzenes are still present, the acyclic isoprenoids have been reduced but not removed, and the PAHs have been reduced. The high resolving power of GC × GC enabled the rapid

determination of microbial degradation of the sample extracts.

GC × GC compound class separations can be very useful for understanding weathering patterns of petroleum and quantifying the influence of evaporation, water-washing, and other processes on residual oil composition. For example, in Figure 5-13 an enlarged portion of the volatility-by-polarity GC × GC chromatogram of the West Falmouth sediment extract is shown along with GC × GC chromatograms of neat Marine Ecosystems Research Laboratory (MERL) No. 2 fuel oil, and MERL oil that has been evaporatively weathered to lose 30% and 70% by mass. When compared to the neat MERL oil, the sediment extract chromatogram has some obvious differences that are due to differences in chemical composition as well as visual scaling. For example, the MERL oil has abundant *n*-alkanes, so the rest of the image is scaled to the *n*-alkanes and the rest of the peaks appear small. The sediment extract has no large *n*-alkane peaks, so smaller peaks are a greater percentage of the mixture, and appear larger than in the MERL oil chromatogram. Therefore, peaks from compounds such as phenanthrenes are more prominent in the sediment extract chromatogram than in the MERL oil chromatogram.

Comparisons between the sediment extract and MERL oil chromatograms in Figure 5-13 show that the *n*-alkanes and more volatile water soluble (polar) compounds have been preferentially lost, but the mechanism of loss is not easily explained by simple evaporative weathering, water-washing, or biodegradation. For example, the 30% evaporatively weathered MERL oil shows a loss of hydrocarbons less than that of *n*-C_{10} that is similar to that shown in the sediment extract. However, the 30% weathered MERL oil contains abundant C_1-naphthalene (C1N) and C_2-naphthalene (C2N) compounds that are noticeably absent in the sediment extract chromatogram. Not until the MERL oil is evaporatively weathered to 70% by mass are the C_1- and C_2-naphthalene compounds removed. At the same time, that degree of weathering removed all other hydrocarbons more volatile than *n*-C_{14} that is not observed in the sediment extract. Thus, it is clear that simple evaporative weathering cannot solely describe the GC × GC pattern observed in the lower-molecular-weight components of the spilled oil found in the Wild Harbor sediment. One contributing mechanism appears to be a preferential loss of the more polar and water-soluble alkylnaphthalenes without the concurrent loss of nonpolar alkanes in the sediment extract. Such a loss may be due to the combined affects of water-washing or preferential biodegradation of more polar compounds.

5.3.3 Winsor Cove No. 2 Fuel Oil Spill

In this application, GC × GC with mass spectrometric detection (GC × GC-TOFMS) found that alkyl decalins (decahydronaphthalenes) are a class of petroleum compounds that are surprisingly persistent in the environment after a spill.

On October 9, 1974, the fuel barge *Bouchard 65* spilled an undetermined amount of No. 2 fuel oil off the west entrance of the Cape Cod Canal. The spilled oil contaminated the Winsor Cove salt marsh located within the Buzzards Bay estuary in Bourne, Mass. (Figure 5-14). To assess the long-term effects of the spilled oil, a core sample of sediment from Winsor Cove was taken in 2001. The sample contained extractable and measurable oil in the upper 4 cm of the sediment.

Analysis of the sediment extract by conventional GC shows a UCM characteristic of a degraded petroleum fuel, shown in Figure 5-15A. When the same sediment extract sample was analyzed by volatility-by-polarity GC × GC-FID, as shown in Figure 5-15B, the absence of normal alkanes and the significant reduction in aromatic hydrocarbons suggest the primary mechanisms of weathering were biodegradation and water-washing (Reddy et al., 2002). The presence of several large peaks in the cyclic alkane regions of the GC × GC chromatogram was noted, and a follow-up study using GC × GC with time-of-flight mass spectrometric detection (GC × GC-TOFMS)

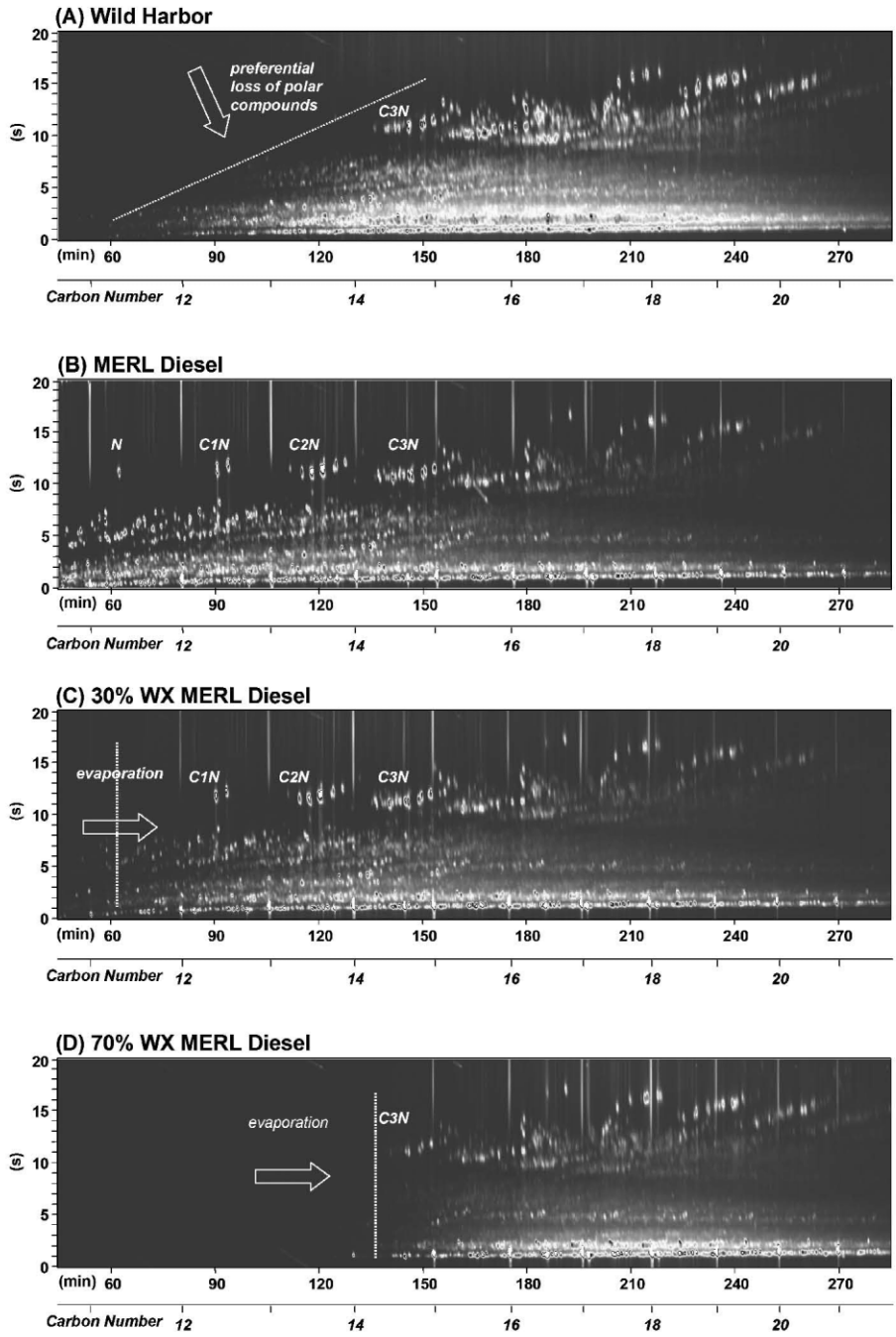

Figure 5-13 Comparison of Wild Harbor sediment extract with weathered MERL oil: (A) Enlarged volatility-by-polarity GC × GC chromatogram of Wild Harbor extract, Aug. 2000 (as in Figure 5-12); (B) neat MERL oil; (C) 30% by mass weathered (WX) MERL oil; (D) 70% by mass weathered (WX) MERL oil. The first column separation along the *x*-axis was accomplished using a nonpolar polydimethylsiloxane stationary phase. The second column separation was accomplished using a polar 14%-cyanopropylphenyl polysiloxane stationary phase. Weathering experiments were performed in a hood where neat MERL oil was allowed to evaporate until the desired mass loss was achieved. The background is blue. Peak intensity is scaled from white, to red, and then to blue (most intense). Compound abbreviations: (N) naphthalene; (C1N) C_1-naphthalenes; (C2N) C_2-naphthalenes; (C3N) C_3-naphthalenes. Reprinted with permission from Reddy et al., 2002. Copyright 2002, American Chemical Society. See color plate.

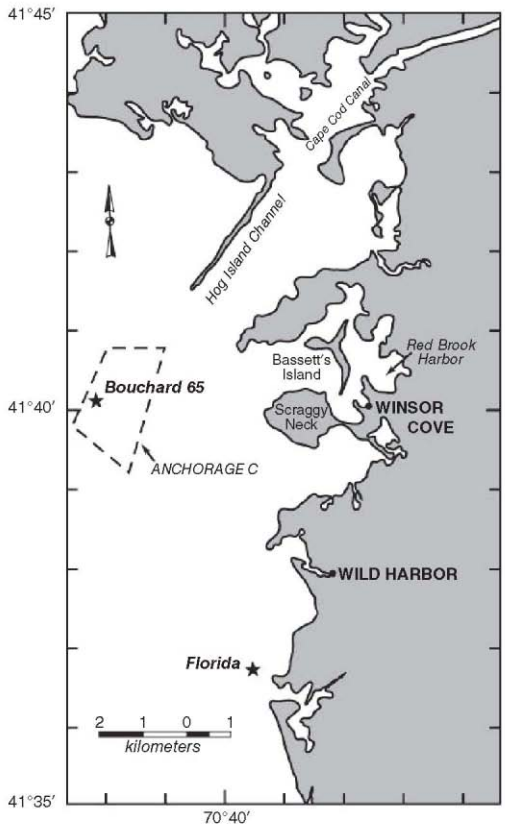

Figure 5-14 Map of the general area near the grounding of the barge *Bouchard 65*. The grounding of the barge *Florida*, discussed previously, is also shown for reference.

determined these compounds to be from the bicyclic sesquiterpanes class of petroleum constituents, most likely pentamethyl- or hexamethyl-substituted decahydronaphthalenes, or hexamethyloctahydroindenes. A comparison of peaks in Figure 5-15(A) with the drimane-based sesquiterpanes identified by Stout et al. (2005) shows a high degree of similarity. Figure 5-16 shows some examples of these compounds, also known as the C_5- and C_6-decalins (Wang et al., 2005). Bicyclic sesquiterpanes such as the C_4- and C_6-decalins have boiling points within the diesel range and are common in oils (Stout et al., 2005; Wang et al., 2005).

The discovery of an archived sample of neat *Bouchard 65* No. 2 fuel oil provided additional opportunities to study the long-term fate of recalcitrant compounds like the C_4- to C_6-decalins. Neat *Bouchard 65* fuel oil was incubated in an aerobic, nutrient-rich environment in the laboratory, and the oil composition was directly compared to the oil found in the sediments at Winsor Cove after 30 years of *in situ* degradation. To illustrate compositional changes in the *Bouchard 65* incubations over time, representative GC-FID chromatograms of the laboratory-degraded oil from three time points are shown in Figure 5-17. Prevalent *n*-alkane and branched alkane peaks apparent in day 1 [Figure 5-17(A)] are significantly smaller by day 11 [Figure 5-17(B)] and nearly indiscernible from the UCM by day 46 [Figure 5-17(C)] of the experiment.

To investigate the effect of weathering and biodegradation on the C_4- to C_6-decalins, volatility-by-polarity GC × GC-TOFMS was used. Figure 5-18 shows GC × GC *m/z* 123 extracted ion chromatograms (EICs) in the region of the target compounds from incubation time 0–46 days and the Winsor Cove sediment extract taken approximately 30 years after the spill. Ion *m/z* 123 is known to be common in the fragmentation pattern of various C_4- to C_6-decalin isomers. The pattern of alkyl decalin peaks in each EIC in Figure 5-18 is similar to that found by Stout et al. (2005) and Wang et al. (2005) using GC-MS, except GC × GC-TOFMS has the advantage of tiling each homologous series of alkyl decalins (C_4-, C_5-, and C_6-decalins) into separate bands. To illustrate this, in Figure 5-18(F), the C_4- to C_6-decalin bands are labeled along with the position of two representative compounds whose structures are shown in Figure 5-16. Peak A is 8β(H)-drimane, a C_5-decalin (C5D). Peak B is 8β(H)-homodrimane, a C_6-decalin (C6D).

Looking at Figures 5-18(A)–(D), there is little change in the distribution and sizes of peaks in the target region as the degradation progresses to 46 days incubation. Figure 5-18(E) shows a day-46 sample spiked with a C_5-decalin standard containing both cis- and trans-1,1,4,4,6-pentamethyldecalin. The standard confirmed the location of the target compounds by producing peaks within the target

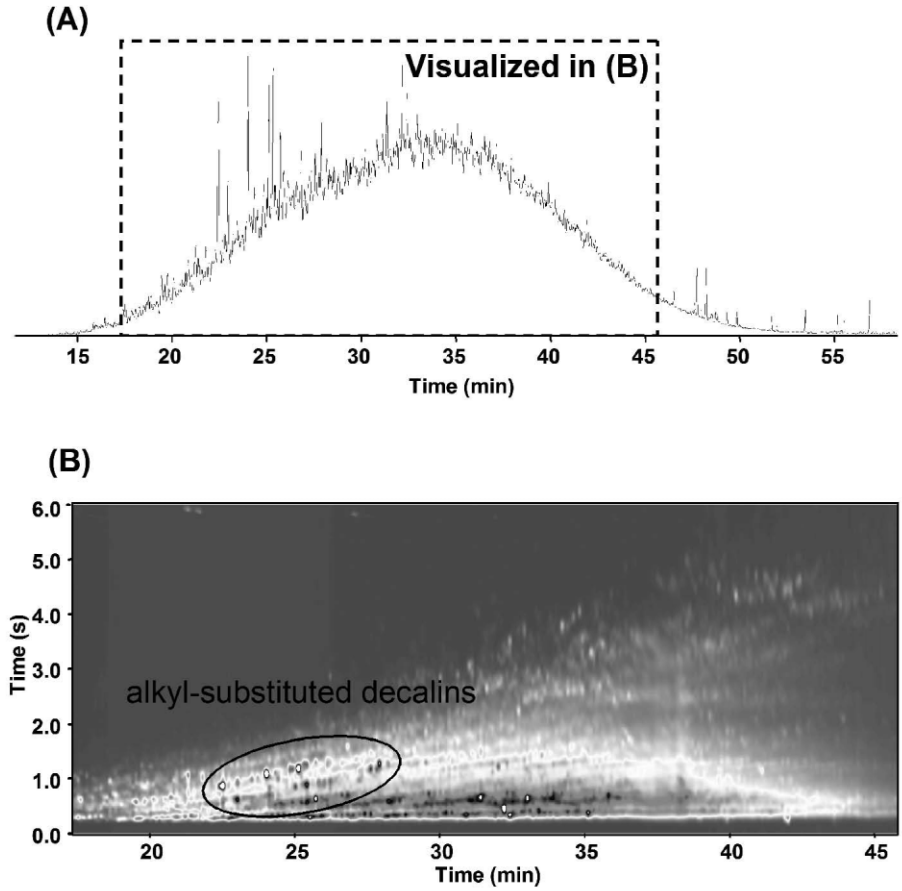

Figure 5-15 Chromatograms of the sediment extract taken from Winsor Cove in 2002 approximately 30 years after being contaminated with No. 2 fuel oil: (A) one-dimensional gas chromatogram showing UCM and the region of the chromatogram visualized in (B). The separation was accomplished using a polydimethylsiloxane stationary phase; (B) volatility-by-polarity GC × GC-FID chromatogram showing the region containing the target compounds. The first-column separation shown along the *x*-axis was accomplished with a polydimethylsiloxane stationary phase. The second-column separation shown along the *y*-axis was accomplished with a 50%-phenylpolysilphenylene-siloxane stationary phase. See color plate.

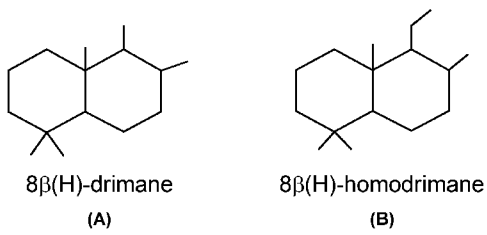

Figure 5-16 Possible structure of C_5- and C_6-decalins found in degraded No. 2 fuel oil in Winsor Cove approximately 30 years after a spill: (A) 8β(H)-drimane; (B) 8β(H)-homodrimane.

compound band in the GC × GC chromatogram. The very large standards peaks made the other peaks seem smaller so they appear slightly different from the same peaks in the other chromatograms. Figure 5-18(F) is the Winsor Cove sediment extract GC × GC chromatogram. The distribution and sizes of peaks in the Winsor Cove GC × GC chromatogram are very similar to that of the day-46 chromatogram, suggesting little if any change in the amounts of these target compounds during weathering or biodegradation conditions encountered by these samples over time.

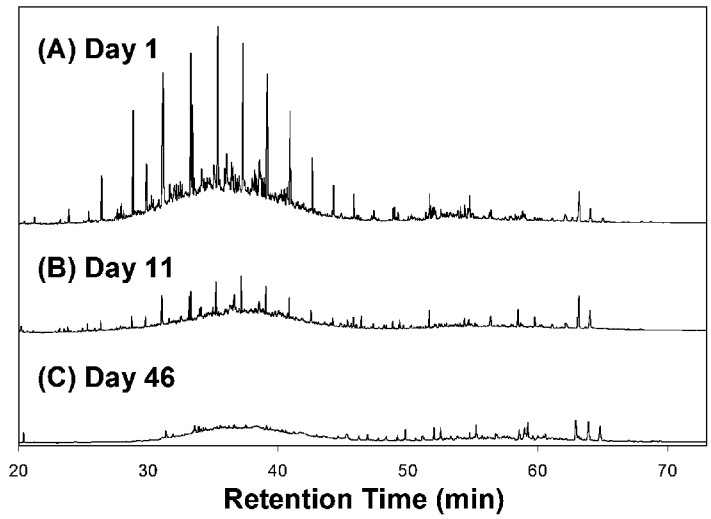

Figure 5-17 Gas chromatograms of *Bouchard 65* incubation sediment extracts artificially degraded in the laboratory: (A) day 1; (B) day 11; (C) day 46.

The recalcitrance of alkyl decalins despite a loss of equally and less volatile compounds in the laboratory degradation experiment as well as that observed in long-term field studies leads to the question of why the alkyl decalins are especially persistent. Structural complexity may limit the availability of these compounds to microorganisms, as the methyl groups surrounding the decalin backbone appear to serve as protection from microbial degradation. The high-resolution separation of these compounds from the UCM by GC × GC and GC × GC-TOFMS may provide additional information relevant to the distribution of these compounds and thus their potential usefulness in fingerprinting methods. For example, in Figure 5-18, the GC × GC *m/z* 123 ion chromatograms show the separation of alkyl decalin compounds that would have been unresolvable in a GC-MS analysis.

5.3.4 Buzzards Bay No. 6 (Bunker C) Spill

In this application, GC × GC was able to track the compositional changes due to weathering processes of a spilled No. 6 fuel oil over a 6-month period. Along with standard GC × GC analysis, unique data visualization techniques elucidated compositional changes due to evaporation, water-washing, and biodegradation (Nelson et al., 2006).

On April 25, 2003, the petroleum cargo barge *Bouchard 120* struck an underwater ledge and released ~375,000 liters of petroleum into Buzzards Bay, Mass., USA (Figure 5-19). Within 24 hours, helicopter surveys documented a 20-km slick that eventually impacted ~150 km of shoreline along the west, north, and northeast shorelines of Buzzards Bay.

The cargo aboard the *Bouchard 120* was No. 6 fuel oil, also known as Bunker C. This type of oil is a residual fuel that is prepared from the remaining hydrocarbons after the lighter constituents of crude oil have been removed at the refinery (Stout et al., 2002). (See also Chapter 10 herein.) The *Bouchard 120* cargo oil contained compounds with an *n*-alkane range from *n*-C_{10} to greater than *n*-C_{45}; however, most of the GC-detectable mass resides in an elution window between *n*-C_{14} and *n*-C_{35}. The *Bouchard 120* cargo also contained abundant alkylated naphthalenes and phenanthrenes that were present in this fuel oil as a result of the addition of a cutting agent used to aid in the transport and delivery of the viscous product.

Figures 5-20(A) and 5-20(C) show traditional gas chromatograms of extracts from

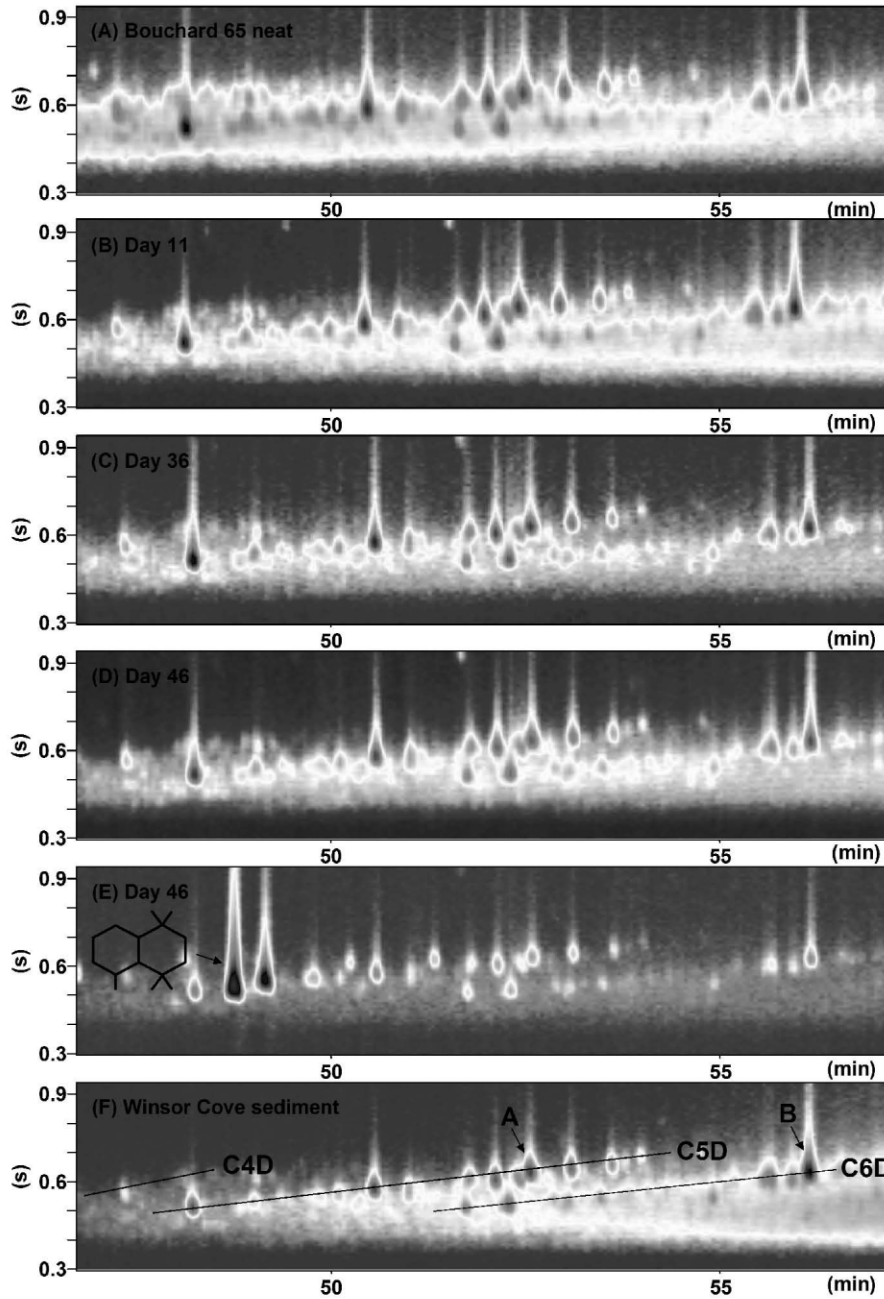

Figure 5-18 Volatility-by-polarity GC × GC m/z = 123 extracted ion chromatographs of *Bouchard 65* incubation sediment extracts showing the C_4- to C_6-decalin region: (A) neat *Bouchard 65* fuel oil; (B) day 11; (C) day 36; (D) day 46; (E) day 46 spiked with cis- and trans-1,1,4,4,6-pentamethyldecalin standard; (F) Winsor Cove sediment extract showing the bands of peaks containing C_4-decalins (C4D), C_5-decalins (C5D), C_6-decalins (C6D), and location of 8β(H)-drimane (A) and 8β(H)-homodrimane (B) whose structures are given in Figure 5-16. The first-column separation shown along the *x*-axis was accomplished with a nonpolar polydimethylsiloxane stationary phase. The second-column separation shown along the *y*-axis was accomplished with a polar 50%-phenylpolysilphenylene-polysiloxane stationary phase. See color plate.

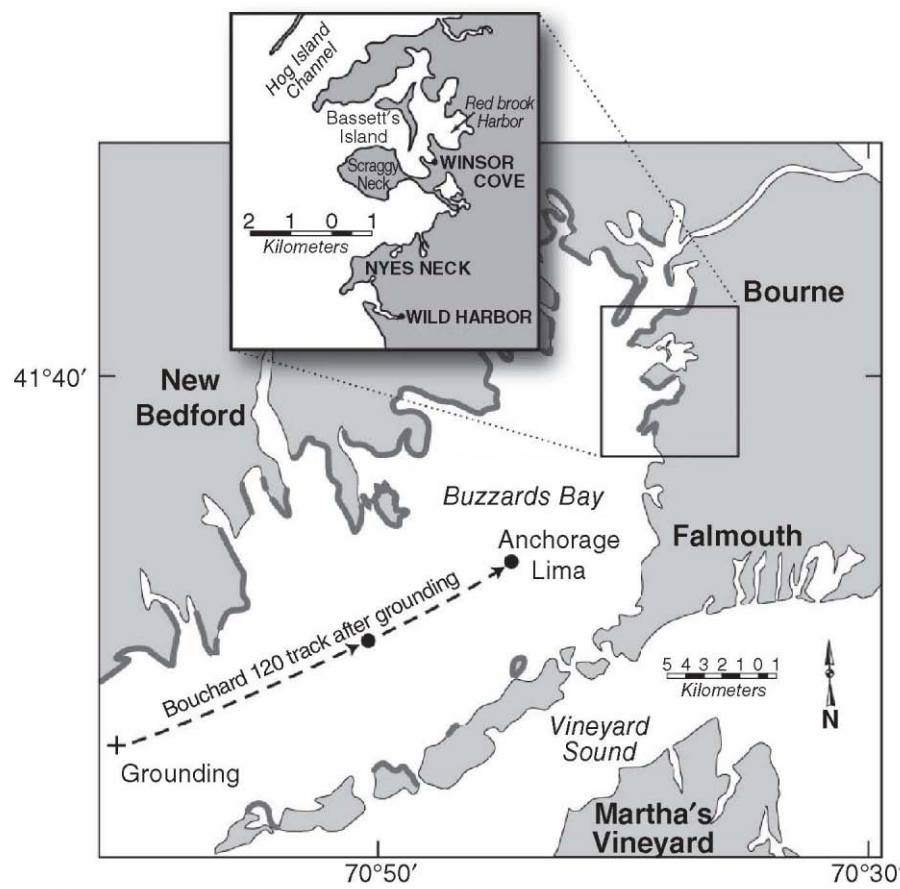

Figure 5-19 Map of Buzzards Bay showing the track of the *Bouchard 120* barge on April 27, 2003. Oil-impacted beaches are highlighted in gray around the perimeter of the bay. Nyes Neck (where the oil spill samples discussed in this section were collected) is shown on the inset map. Copyright 2006 from *Tracking the Weathering of an Oil Spill with Comprehensive Two-Dimensional Gas Chromatography*, by Nelson et al. Reproduced by permission of Taylor & Francis Group, LLC., http://www.taylorandfrancis.com.

oil-covered rocks collected at Nyes Neck on May 9, 2003, and on November 23, 2003, 12 days and 179 days, respectively, after the initial release of No. 6 fuel oil into Buzzards Bay. These dates span the temporal range of samples collected at Nyes Neck. The chromatograms reveal a complex mixture of hydrocarbons that elutes mainly between n-C_{15} and n-C_{37}. Significant differences in these chromatograms are apparent. For example, the n-alkane peaks, which were prominent in the day-12 chromatogram, are not discernable in the day-179 chromatogram. These changes are likely due to the combined weathering effects of biodegradation, water-washing, and evaporation. The end result of nearly six months of weathering is a mixture of petroleum hydrocarbons that is in the form of a broad UCM hump in the conventional gas chromatogram (Figure 5-20C).

The tremendous resolving power of GC × GC and ordered separation of peaks in the GC × GC chromatogram helps identify more detailed compositional changes in the No. 6 fuel oil that occurred during weathering that cannot be seen using traditional gas

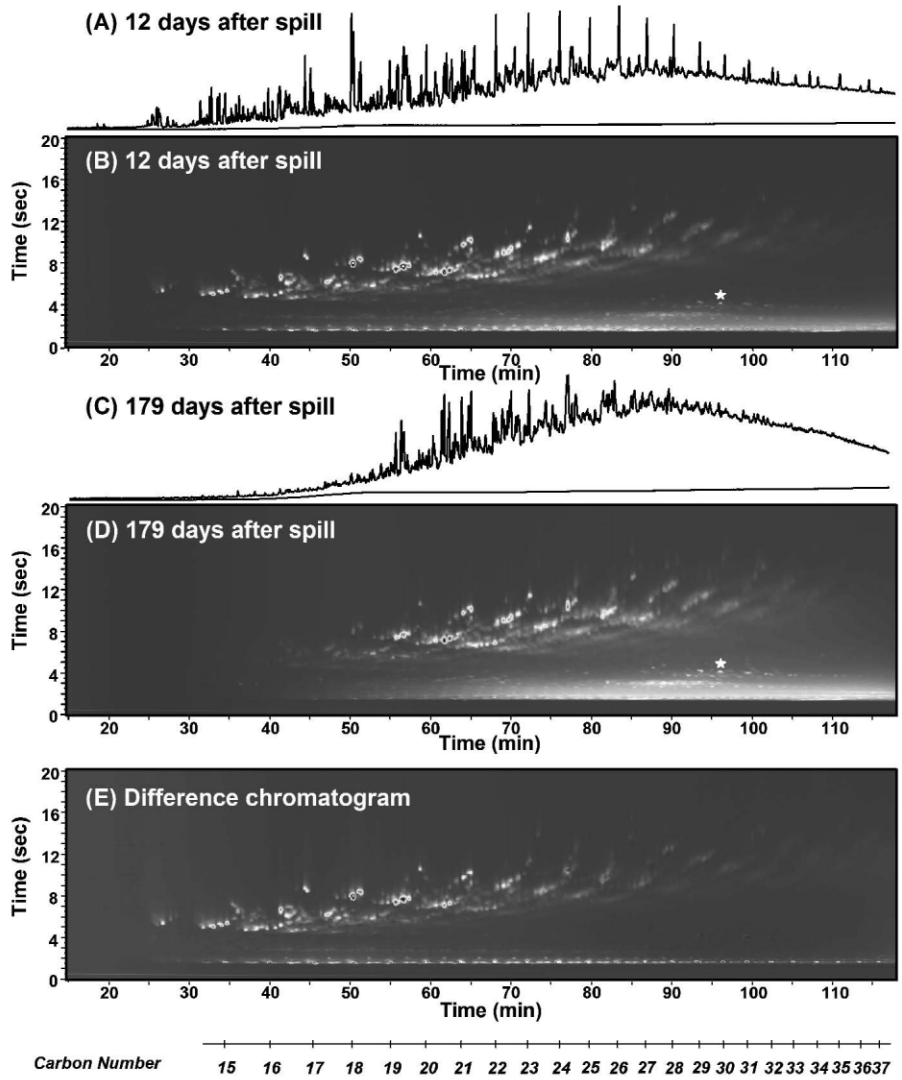

Figure 5-20 Conventional GC and GC × GC chromatograms of sample extracts from *Bouchard 120* No. 6 fuel oil-covered rocks collected at various times after the spill: (A) conventional GC chromatogram of sample taken 12 days after the spill. The separation was achieved using a polydimethylsiloxane stationary phase; (B) GC × GC volatility-by-polarity chromatogram of sample taken 12 days after the spill. The first dimension separation along the *x*-axis was achieved using a nonpolar polydimethylsiloxane stationary phase. The second dimension separation along the *y*-axis was achieved with a polar 50% phenylpolysilphenylenesiloxane stationary phase; (C) conventional GC chromatogram of sample taken 179 days after the spill; (D) GC × GC volatility-by-polarity chromatogram of sample taken 179 days after the spill; (E) a point-by-point difference chromatogram produced by the subtraction of chromatogram (D) from chromatogram (B) after normalization to the conserved standard 17α(H)-21β(H)-hopane (marked with a star). Copyright 2006 from *Tracking the Weathering of an Oil Spill with Comprehensive Two-Dimensional Gas Chromatography*, by Nelson et al. Reproduced by permission of Taylor & Francis Group, LLC., http://www.taylorandfrancis.com.

chromatograms. To illustrate, GC × GC chromatograms for day 12 and day 179 are visualized as interpolated color contour plots in Figures 20(B) and 20(D) respectively. Each chromatogram is normalized and scaled to the conserved biomarker 17α(H)-21β(H)-hopane (Prince et al., 1994) indicated on the plots with a star. Extreme differences in the hydrocarbon composition between day 12 and day 179 are readily apparent throughout the chromatogram. It is possible to identify the chemical classes affected by weathering because petroleum compound classes occupy specific regions of the chromatogram (see Figs. 5-5 and 5-7). For example, most of the alkylated naphthalene and phenanthrene compound peaks eluting before *n*-C_{18} were lost between day 12 and day 179.

More advanced image processing tools improve data analysis by extracting trends from complex data. In the spill case described here, plots using chromatogram difference, ratio, and addition quantitatively compared point-by-point the difference between two samples that span almost six months of degradation by various weathering processes (Nelson et al., 2006). The differences found, in turn, provide valuable information about the effect of the various weathering processes on the numerous chemical classes found in the petroleum samples. For example, Figure 5-20(E) shows the resulting chromatogram that is generated when the heavily weathered day-179 chromatogram is subtracted from the slightly weathered day-12 chromatogram. The difference chromatograms provide a way to identify compound peaks that have changed in volume relative to 17α(H)-21β(H)-hopane over this six-month weathering time frame. Peaks appearing in the GC × GC difference chromatogram (Fig. 5-20E) are those that lost peak volume through weathering, with prominent peaks indicating a large loss and small peaks indicating a small loss. Over the six-month weathering period, the *n*-alkanes and the alkylated naphthalenes showed a significant loss of peak volume, while the branched alkanes, located in between the *n*-alkanes, showed a small loss. The sterane and hopane peaks showed little or no loss as evidenced by a lack of peaks in this region of the difference chromatogram. See Figure 5-7 for the location of these petroleum compound classes in the chromatogram.

To produce good results, peaks for compounds in both chromatograms must have the same first- and second-dimension retention times. Run-to-run retention time reproducibility is generally found acceptable for visual comparisons. Rigorous peak matching needed for more robust quantitative and chemometric comparisons can be facilitated by use of special algorithms (Johnson et al., 2003; Ni et al., 2005). (See also Chapter 9 herein.)

GC × GC chromatogram comparisons such as that employed above identify target chemical classes that are both affected and unaffected during weathering processes. The improved separation by GC × GC of target chemical classes from one another allows the use of a flame ionization detector to quantify the loss of target classes during weathering. Figure 5-21 is a comparison of the relative percent loss for a homologous series of *n*-alkanes, *n*-alkylcyclohexanes, and some isoprenoid branched alkanes. The data are presented by retention index because compounds that have the similar retention indices are assumed to have similar tendencies to evaporate. Since these saturates have very low water-solubilities (Eastcott et al., 1988), they all should be affected by water-washing in a comparable manner. The *n*-alkanes have a near constant loss of 90–100% for retention indices of 1500–2000 and then an ordered dropoff to only 20% loss at retention index of 3600. The *n*-alkylcyclohexanes only have 30–60% loss in the retention indices of 1500–2000 and a nearly constant loss of 15% from 2100–2600. The differences in weathering loss between these compounds with similar tendencies to evaporate and dissolve may provide a means to discriminate weathering patterns. In this case, these results show how susceptible *n*-alkanes are to biodegradation relative to *n*-alkylcyclohexanes once the evaporation component is removed.

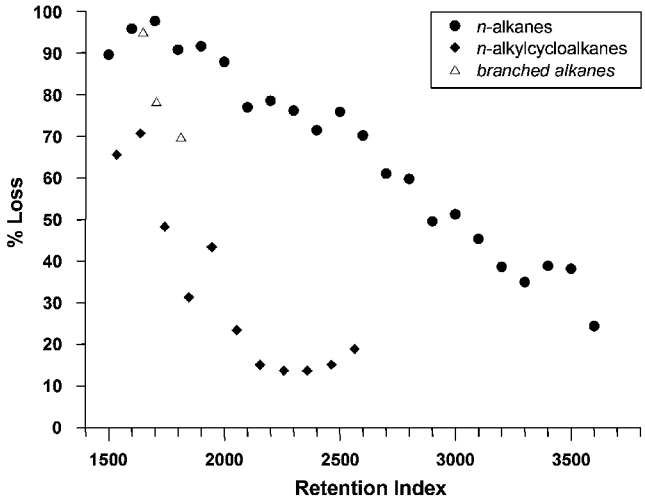

Figure 5-21 Percent losses of select hydrocarbons from *Bouchard 120* No. 6 fuel oil covered rocks collected at Nyes Neck after six months of weathering: (●) *n*-alkanes; (◆) *n*-alkylcyclohexanes; (△) branched alkanes. Copyright 2006 from *Tracking the Weathering of an Oil Spill with Comprehensive Two-Dimensional Gas Chromatography*, by Nelson et al. Reproduced by permission of Taylor & Francis Group, LLC., http://www.taylorandfrancis.com.

5.3.5 Oil Seeps, Santa Barbara, CA, USA

In this final application, GC × GC identifies compositional changes between a reservoir sample of crude oil taken at a Santa Barbara, CA, USA, oil platform and a sample of oil that seeped from a nearby underwater fault zone. The Santa Barbara well sample exhibits unique isoprenoid alkane, hopane, and sterane biomarker chemical signatures that distinguish these oils from other crude oils from around the world.

The offshore Santa Barbara region is known for its very active oil seeps (Hornafius et al., 1999). Carbon-rich marine Miocene sediments provide the source material for the generation of oil in this area (Hornafius et al., 1999; Reed and Kaplan, 1977). Uranium-Thorium (U-Th) measurements of calcite cements around areas where hydrocarbons are believed to have seeped to the surface in the past suggest that hydrocarbons have been moving along faults around the rim of the basin for the past 120,000 and perhaps up to 500,000 years before the present (Boles et al., 2004). Widespread seepage of hydrocarbons occurs along offshore fault zones in the waters of the Santa Barbara basin. Estimates of the amount of hydrocarbons migrating into the environment by way of the natural seeps around Coal Oil Point put the combined gas–liquid hydrocarbon seepage flux at approximately 37 tons per day, with methane emissions comprising 65% of this total (24 tons per day) (Quigley et al., 1996, 1999; Washburn et al., 1996). The volume of gas emanating from the seeps has been fluctuating over time. The fluctuations are most likely linked to daily tidal cycles, oil production at the nearby Holly platform, and seismic activity along the faults in Santa Barbara county (Boles et al., 2001; Leifer et al., 2004).

Modern scientific investigations of the Santa Barbara oil/methane seeps began in earnest during the middle of the 20th century. Some of the earliest GC separations of hydrocarbons upwelling in the Santa Barbara channel date back to 1973 (Mikolaj, 1973). The resolving power of GC coupled to mass spectrometers advanced the study of oil from these seep areas (Kaplan and Reed, 1977; Stuermer et al., 1982). Some of the many chemical structures of compounds extracted from these seep oils were assigned using this approach.

More recent efforts have focused on analyzing seep fluids for the presence and ratios of biomarkers to determine the possible reservoir sources and transport directions of the fluids. Targeted compounds or their ratios typically include trisnorhopane, sterane/hopane ratios, refractory index, C_{28}/C_{29} hopane ratios (Kvenvolden, 2004). Other researchers study-

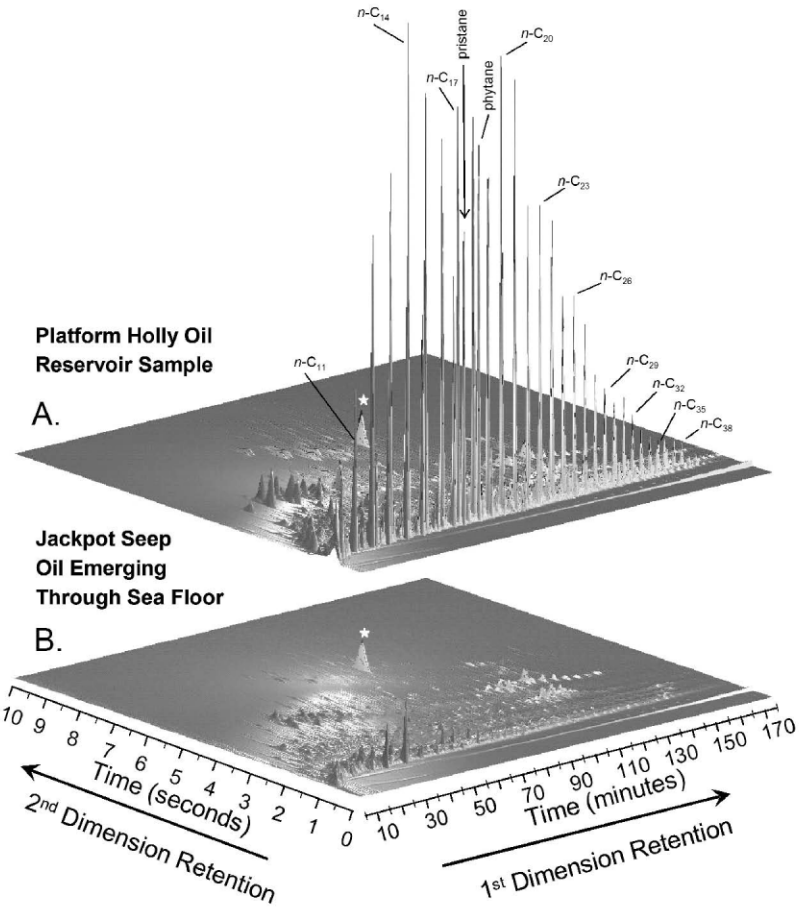

Figure 5-22 Volatility-by-polarity GC × GC chromatogram of (A) reservoir crude oil from platform Holly, Santa Barbara Channel, California, and (B) oil stringer emerging through the sea floor collected at the Jackpot seep field, Santa Barbara Channel, California. The first-column separation shown along the *x*-axis was accomplished with a nonpolar polydimethylsiloxane stationary phase. The second-column separation shown along the *y*-axis was accomplished with a polar 50%-phenylpolysilphenylene-siloxane stationary phase. A star on each chromatogram indicates the position of the internal standard dodecahydrotriphenylene (DDTP). The distinct difference in *n*-alkane content between the two samples is evident in this figure. See color plate.

ing the toxicological effects of seep fluids on marine organisms have measured PAHs (Davis et al., 1981; Spies et al., 1980; Stuermer et al., 1981; Seruto et al., 2005). Geochemical tracing of tarballs from these seeps have been investigated as well (Hostettler et al., 2004). All this work has been limited to traditional GC, which is a technology that is at least two decades old and has provided a limited number of analytes.

To compare the differences in the reservoir composition of crude oil from platform Holly to what is naturally seeping out along coastal Santa Barbara, a series of samples was collected and analyzed by GC × GC. Figure 5-22 shows two volatility-by-polarity GC × GC chromatograms visualized as mountain plots. In (A), the reservoir sample of oil from the platform Holly exhibits the typical inventory of alkane and aromatic constituents. In (B), the sample was from an oil stringer emerging through the sea floor at Jackpot Seep, in close proximity to platform Holly. The star in each chromatogram indicates the position of the

internal standard dodecahydrotriphenylene (DDTP) that was added to each sample. Both of the chromatograms were normalized to the peak volume of 17α(H), 21β(H)-hopane, a known conserved biomarker used in monitoring oil weathering processes when crude oil is released into the environment (Prince et al., 1994).

These images reveal the substantial scope and scale of the changes that occur in crude oils due to processes that act on a localized petroleum system, provided that the source oil for the seep and Holly are genetically related. The major differences between the reservoir and seafloor samples appear to occur in the relative abundances of the naphthalene peaks, the branched and isoprenoid alkane peaks, and most noticeably in the normal alkane peaks.

Another feature of Holly oil, like all oils from Monterey shale and carbonate source rocks, is the unique biomarker chemical signatures that distinguish these oils from other types of crude oils worldwide. For example, they may contain several biomarkers derived from Archaea (Orphan et al., 2001). Since their discovery and subsequent classification as a third domain of life on earth (Brock and Freeze, 1969; Brock et al., 1972; Woese and Fox, 1977), members of the domain Archaea are often thought to be nature's "extremists" as they exist in hot springs, deep subsurface sediments, strongly acidic and alkaline springs, volcanic vent systems, extremely saline evaporitic environments, and deep-sea hydrothermal vent systems. Members of the domain Archaea have also been shown to be abundant in picoplankton of open ocean environments as well (DeLong, 1992; DeLong et al., 1998, 1999). However, most Archaea are thermophilic, and many are extremely thermophilic with optimum growth temperatures between 80° and 115°C.

One of the defining characteristics of the Archaea and the source of their usefulness as biomarkers is the unique membrane lipids of this group. The membrane lipids of Archaea are very different than either the eukaryotes or the prokaryotic bacteria. Archaean lipid membranes form a monolayer not a bilayer as in bacteria and eukaryotes (De Rosa et al., 1980; Kates, 1993; Koga et al., 1993). Archaeal lipid membranes are ether-linked (not ester-linked) to glycerol with C_{20} to C_{40} branched isoprenoid alkane moieties spanning the glycerol units at each end (De Rosa et al., 1980). In the most thermophilic species (the Chrenarchaea), the lipid membranes consist of C_{40} isoprenoid lipids that are thought to reduce the fluidity of the cell membranes at extreme temperatures (De Rosa et al., 1980). The presence of these unique lipid compounds in a geological sample is strong evidence of Archaean activity either in the deep sediments, in the oil reservoirs, or along the path that migrating oil takes as it makes its way through fractures and faults between the reservoirs and the sea floor. Figure 5-23 highlights the region of a GC × GC chromatogram of the Platform Holly produced crude oil where these Archaean biomarkers elute. Along with a suite of acyclic isoprenoid alkanes, trace amounts of two-ring and three-ring cyclic isoprenoid alkanes are present in this sample as well. The peak assignments were made by comparison with a sample rich in cyclic isoprenoid alkanes obtained from argillitic sediments collected in a gold mine in Timmons, Onatario, Canada (data not shown) (Nelson et al., 2005). Biphytane is the largest of the isoprenoid alkanes in this region of the chromatogram. One of the remarkable features of this part of the chromatogram is how well biphytane and the *n*-C_{35} alkane are resolved from one another.

One of the most striking features of the mid-Miocene Monterey crude oils found at platform Holly is the abundance and distribution of the C_{27}, C_{28}, and C_{29} desmethylsteranes as shown in Figure 5-24. The desmethylsteranes are the most abundant steranes in Monterey Formation-derived crude oils. This is true for many other types of oil as well. Since steranes are derived from sterol precursors, they represent the molecular remnants of eukaryotic life forms from ancient times. In particular, the desmethylsteranes are representative of microalgae and higher plants (Volkman, 2005), diatoms, green algae, red algae, macroalgae, fungi, and yeast (Brocks and Summons, 2004).

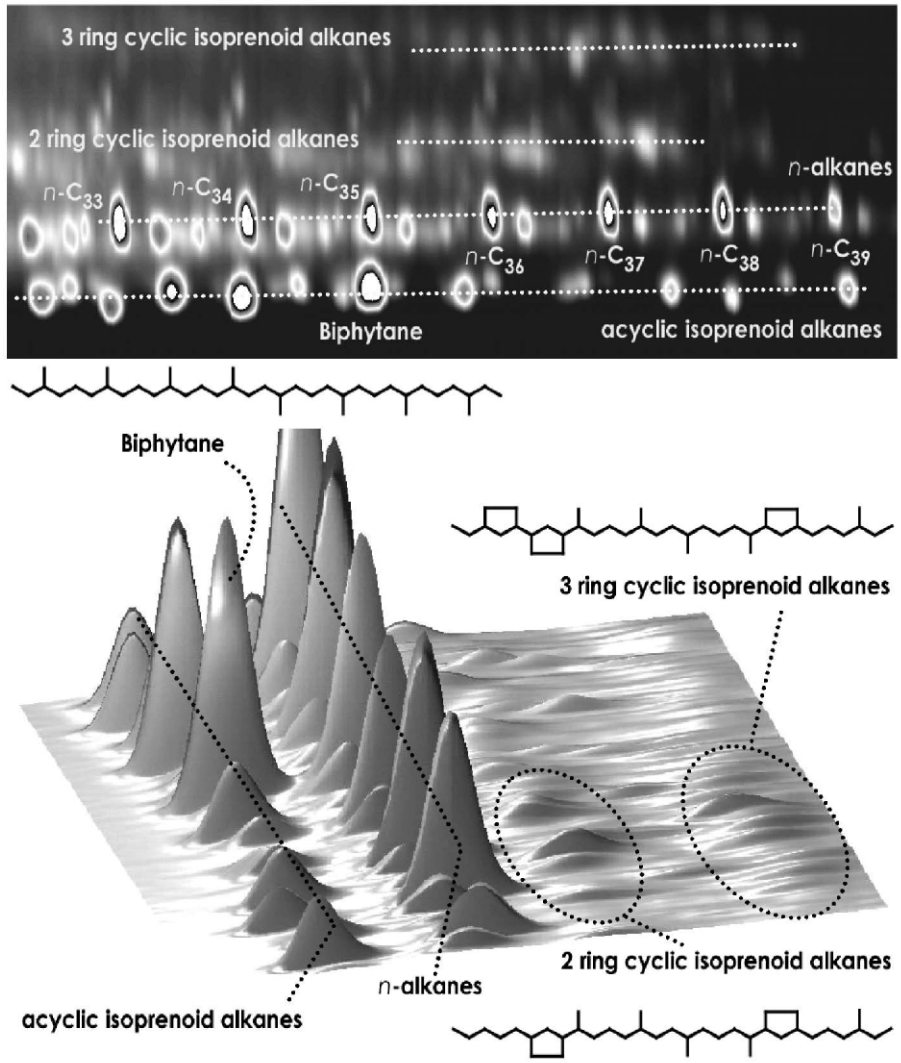

Figure 5-23 Partial volatility-by-polarity GC × GC chromatogram of the platform Holly produced crude oil showing peaks in the vicinity of *n*-C_{33} through *n*-C_{39}. The location of high-molecular-weight isoprenoid alkanes (both acyclic and cyclic), thought to be biomarkers of Archaean membrane lipids, are indicated along with some representative molecular structures. See color plate.

Since C_{27}, C_{28}, and C_{29} desmethylsteranes are derived from a number of marine and terrestrial sources, they are not as useful as depositional source indicators as other biomarkers, but they can provide information about the level of maturation of oil reservoirs (Brocks and Summons, 2004). The identities of the desmethylsterane compounds highlighted in Figure 5-24 are given in Table 5-1. For more discussion of biomarker nomenclature, see Chapter 3 herein.

The presence of hopanes in rock or oil samples is a clear indication of ancient sedimentary bacterial activity (Brocks and Summons, 2004). Monterey shale crude oils contain relatively high concentrations of 28,30-bisnorhopane, a hopanoid that is not ubiquitous in crude oils worldwide (Seifert

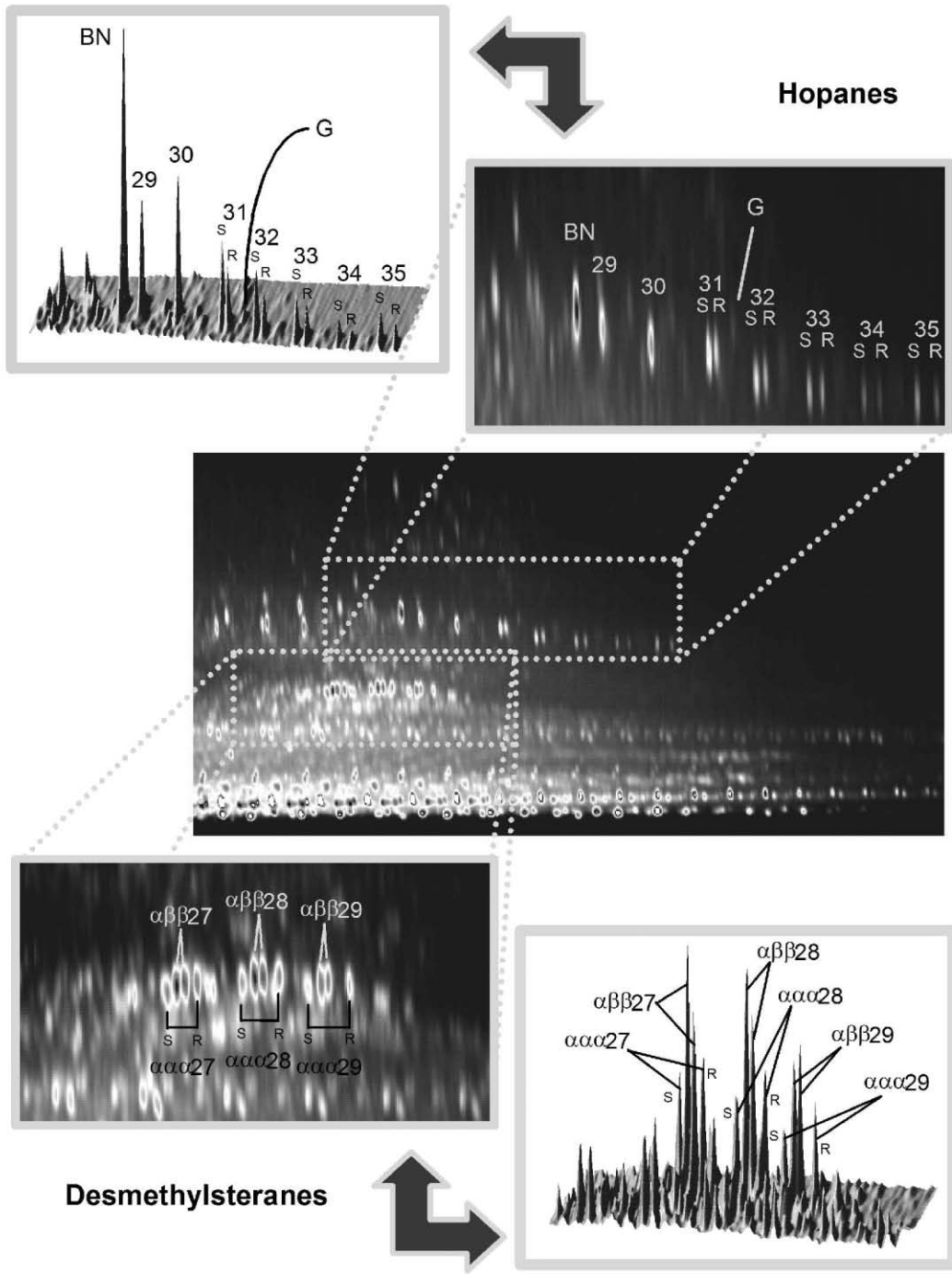

Figure 5-24 Partial volatility-by-polarity GC × GC chromatogram of the platform Holly reservoir crude oil showing peaks in the vicinity of the sterane and desmethylsterane biomarkers. Identification of labeled peaks is found in Table 5-1. See color plate.

Table 5-1 Peak identities of Compounds Labeled in Figure 5-24

Hopane Series Peak Identification	*Compound*
BN	17α(H),18α(H),21β(H)-28,30-bisnorhopane
29	17α(H),21β(H)-29-norhopane
30	17α(H),21β(H)-hopane
31	S & R epimers of 17α(H),21β(H)-29-homohopane
G	gammacerane
32	S & R epimers of 17α(H),21β(H)-29-bishomohopane
33	S & R epimers of 17α(H),21β(H)-29-trishomohopane
34	S & R epimers of 17α(H),21β(H)-29-tetrakishomohopane
35	S & R epimers of 17α(H),21β(H)-29-pentakishomohopane
Desmethylsterane Peak Identification	*Compound*
ααα27	5α(H),14α(H),17α(H)-cholestane
αββ27	5α(H),14β(H),17β(H)-cholestane
ααα28	5α(H),14α(H),17α(H)-ergostane
αββ28	5α(H),14β(H),17β(H)-ergostane
ααα29	5α(H),14α(H),17α(H)-stigmastane
αββ29	5α(H),14β(H),17β(H)-stigmastane

et al., 1978; Curiale et al., 1985). The designations 28 and 30 denote the locations in the 28-carbon bisnorhopane where methyl groups are absent when compared to the corresponding 30-carbon hopane molecule. The presence of high concentrations of 28,30-bisnorhopane in sediments that are marine in origin is indicative of a depositional environment that occurs in a well-stratified water column in which the bottom waters are saline in nature and hydrogen sulfide is present (Grantham et al., 1980; Schoell et al., 1992; Brocks and Summons, 2004). A similar depositional environment exists today in the stratified water column of the Black Sea.

Monterey shale oils typically contain 35-carbon homohopanes (17α(H),21β(H)-29-pentakishomohopane, 22S and 22R epimers) that are present in higher concentration than those of the neighboring 34-carbon homohopanes [17α(H),21β(H)-29-tetrakishomohopane 22S and 22R epimers].

Monterey shale derived oils contain gammacerane, a biomarker associated with hypersaline depositional environments (Moldowan et al., 1985; ten Haven et al., 1988). It is likely that gammacerane could not form from its precursor, tetrahymanol, in oxidizing conditions (ten Haven et al., 1989; Sinninghe Damste, 1995). Considered together, the biomarker distribution suggests that the Monterey Formation sediments were deposited in a euxinic marine environment (Peters et al., 2004a, 2004b; Hostettler et al., 2004), the sediments were deposited below a stratified water column, the bottom water was anoxic, saline, and perhaps even hypersaline, and finally the presence of hydrogen sulfide indicates a reducing sedimentary environment. This is a good example of the type of information that can be obtained by examining the distribution of biomarkers in a crude oil sample. The biomarkers present in a crude oil sample can provide a wealth of diagnostic information about the origin of oil.

Just as GC × GC can help resolve the UCM (Frysinger et al., 2003), GC × GC can also shed additional light on the very complicated sterane patterns obtained by conventional GC-MS. This is demonstrated in the lowest panels shown in Figure 5-24, in which the complex sterane pattern is pulled apart. The large number of small, unidentified peaks reveals the complexity in this suite of compounds, yet GC × GC holds promise to start to unravel this complex mixture.

5.4 Conclusion

There are several advantages that a GC × GC separation offers over a conventional GC separation for the analysis of complex mixtures such as petroleum products and spills. The high resolving power of GC × GC gives a more complete picture of the compounds present in petroleum, so it is easier to detect, identify, and quantify individual compounds and families of compounds present in the sample. Peak quantitation in GC × GC can be accomplished using

a flame ionization detector. GC often requires a mass spectrometric detector operating as a separation mechanism to help with poorly resolved peaks by using extracted ion data, but this approach requires advanced knowledge of target compounds and compound classes. GC × GC enhances the power of a mass spectrometer detector by presenting to the detector a single-component peak so that the mass spectrum does not contain artifacts that can hinder interpretation and confuse library search algorithms. Each of these advantages is particularly relevant to improved methods of oil spill analysis and source identification. New target compounds or classes of compounds that are useful for fingerprinting can be discovered, identified, and quantified to a degree not attainable with conventional GC and GC-MS methods.

Acknowledgments

The authors acknowledge the following people who contributed to the work described in this chapter. From Woods Hole Oceanographic Institution: Lary Ball, Heather Bischel, George Hampson, Emily Peacock, Desiree Plata, Bruce Tripp, Helen White, and Li Xu; from the University of California at Santa Barbara: David Valentine and George Wardlaw; from the University of Illinois: Fabien Kenig and Todd Ventura. The following organizations provided funding for the work described in this chapter: U.S. Department of Energy, U.S. Environmental Protection Agency, National Science Foundation, U.S. Navy Office of Naval Research, Petroleum Research Fund, The Island Foundation, Robert T. Alexander Trust, and National Institute of Justice.

References

ASTM (American Society for Testing and Materials), *Standard Test Methods for Comparison of Waterborne Petroleum Oils by Gas Chromatography*, D-3328-00, 2000a, W. Conshohocken, PA.

ASTM (American Society for Testing and Materials), *Standard Practice for Oil Spill Identification by Gas Chromatography and Positive Ion Electron Impact Low Resolution Mass Spectrometry*, D-5739-00, 2000b, W. Conshohocken, PA.

Beens, J., J. Dallüge, M. Adahchour, R.J.J. Vreuls, and U.A.Th. Brinkman, Moving cryogenic modulator for the comprehensive two-dimensional gas chromatography (GC × GC) of surface water contaminants, *J. Microcolumn Separation*, 2001a, **13**, 134–140.

Beens, J., M. Adahchour, R.J.J. Vreuls, K. van Altena, and U.A.Th. Brinkman, Simple, non-moving modulation interface for comprehensive two-dimensional gas chromatography, *J. Chromatography A*, 2001b, **919**, 127–132.

Bertsch, W., Two-dimensional gas chromatography. Concepts, instrumentation, and applications — Part 1: Fundamentals, conventional two-dimensional gas chromatography, selected applications, *J. High Resolution Chromatography*, 1999, **22**, 647–665.

Bertsch, W., Two-dimensional gas chromatography. Concepts, instrumentation, and applications — Part 2: Comprehensive two-dimensional gas chromatography, *J. High Resolution Chromatography*, 2000, **23**, 167–181.

Blomberg, J., P.J. Schoenmakers, J. Beens, and R. Tijssen, Comprehensive two-dimensional gas chromatography (GC × GC) and its applicability to the characterization of complex (petrochemical) mixtures, *J. High Resolution Chromatography*, 1997, **20**, 539–544.

Blomberg, J., T. Riemersma, M. van Zuijlen, and H. Chaabani, Comprehensive two-dimensional gas chromatography coupled with fast sulphur-chemiluminescence detection: implications of detector electronics, *J. Chromatography A*, 2004, **1050**, 77–84.

Boles, J.R., J.F. Clark, I. Leifer, and L. Washburn, Temporal variation in natural methane seep rate due to tides, coal oil point area, California, *J. Geochemical Res.*, 2001, **106**, 27077–27086.

Boles, J.R., P. Eichhubl, G. Garven, and J. Chen, Evolution of a hydrocarbon migration pathway along basin-bounding faults: Evidence from fault cement, *Amer. Assoc. Petroleum Geologists Bull.*, 2004, **88**, 947–970.

Brock, T.D. and H. Freeze, Thermus aquaticus gen. n. and sp. n., a non-sporulating extreme thermophile, *J. Bacteriology*, 1969, **98**, 289–297.

Brock, T.D., K.M. Brock, R.T. Belly, and R.L. Weiss, Solfolobus: A new genus of sulfur-oxidizing bacteria living at low pH and high temperature, *Archeological Microbiology*, 1972, **84**, 54–68.

Brocks, J.J. and R.E. Summons, Sedimentary hydrocarbons, biomarkers for early life, *Treatise on Geochemistry*, H.D. Holland and K.K. Turekian (eds.), 2004, **8**, 63–115.

Bruckner, C.A., B.J. Prazen, and R.E. Synovec, Comprehensive two-dimensional high-speed gas chromatography with chemometric analysis, *Analytical Chem.*, 1998, **70**, 2796–2804.

Burns, K.A. and J.M. Teal, The West Falmouth oil spill: Hydrocarbons in the salt marsh ecosystem, *Estuarine and Coastal Marine Science*, 1979, **8**, 349–360.

Burns, K.A., S. Codi, and N.C. Duke, Gladstone, Australia field studies: Weathering and degradation of hydrocarbons in oiled mangrove and salt marsh sediments with and without the application of an experimental bioremediation protocol, *Marine Pollution Bull.*, 2000, **41**, 392–402.

Curiale, J.A., D. Cameron, and D.V. Davis, Biological marker disribution and significance in oils and rocks of the Monterey formation, California, *Geochimica et Cosmochimica Acta*, 1985, **49**, 271–288.

Dalluge, J., J. Beens, and U.A.Th. Brinkman, Comprehensive two-dimensional gas chromatography: A powerful and versatile analytical tool, *J. Chromatography A*, 2003, **1000**, 69–108.

Davis, J.M., *Statistical Theories of Peak Overlap; Advances in Chromatography*, 1994, P.R. Brown and E. Grushka (eds.), Marcel Decker, New York, **34**, 109–176.

Davis, P.H., T.W. Schultz, and R.B. Spies, Toxicity of Santa Barbara seep oil to starfish embryos: Part 2. The growth bioassay, *Marine Environmental Research*, 1981, **5**, 287–294.

DeLong, E.F., Archaea in coastal marine environments, *Proc. National Acad. Science, USA*, 1992, **89**, 5685–5689.

DeLong, E.F., L.L. King, R. Massana, H. Cittone, A. Murray, C. Schleper, and S.G. Wakeham, Dibiphytanyl ether lipids in nonthermophilic crenarchaeotes, *Applied and Environmental Microbiology*, 1998, **64**, 1133–1138.

DeLong, E.F., L.T. Taylor, T.L. Marsh, and C.M. Preston, Visualization and enumeration of marine planktonic archaea and bacteria by using polyribonucleotide probes and fluorescent in situ hybridization, *Applied and Environmental Microbiology*, 1999, **65**, 5554–5563.

De Rosa, M., E. Esposito, A. Gambacorta, B. Nicolaus, and J.D. Bu'Lock, Effects of temperature on ether lipid composition of Caldariella acidophila, *Phytochemistry*, 1980, **19**, 827–831.

Eastcott, L., W.Y. Shiu, and D. Mackay, Environmentally relevant physical-chemical properties of hydrocarbons: A review of data and development of simple correlations, *Oil and Chemical Pollution*, 1988, **4**, 191–216.

Fraga, C.G., B.J. Prazen, and R.E. Synovec, Enhancing the limit of detection for comprehensive two-dimensional gas chromatography (GC × GC) using bilinear chemometric analysis, *J. High Resolution Chromatography*, 2000, **23**, 215–224.

Frysinger, G.S. and R.B. Gaines, Comprehensive two-dimensional gas chromatography with mass spectrometric detection (GC × GC-MS) applied to the analysis of petroleum, *J. High Resolution Chromatography*, 1999, **22**, 251–255.

Frysinger, G.S. and R.B. Gaines, Separation and identification of petroleum biomarkers by comprehensive two-dimensional gas chromatography, *J. Separation Science*, 2001, **24**, 87–96.

Frysinger, G.S. and R.B. Gaines, Forensic analysis of ignitable liquids in fire debris by comprehensive two-dimensional gas chromatography, *J. Forensic Science*, 2002, **47**, 471–482.

Frysinger, G.S., R.B. Gaines, and C.M. Reddy, GC × GC — A new tool for environmental forensics, *Environmental Forensics*, 2002, **3**, 27–34.

Frysinger, G.S., R.B. Gaines, L. Xu, and C.M. Reddy, Resolving the unresolved complex mixture in petroleum-contaminated sediments, *Environmental Science and Technology*, 2003, **37**, 1653–1662.

Gaines, R.B., G.S. Frysinger, M.S. Hendrick-Smith, and J.D. Stuart, Oil spill source identification by comprehensive two-dimensional gas chromatography, *Environmental Science and Technology*, 1999, **33**(12), 2106–2112.

Gaines, R.B. and G.S. Frysinger, Temperature requirements for thermal modulation in comprehensive two-dimensional gas chromatography, *J. Separation Science*, 2004, **27**, 380–388.

Giddings, J.C., Sample dimensionality: A predictor of order-disorder in component peak distribution in multidimensional systems, *J. Chromatography A*, 1995, **703**, 3–15.

Gorecki, T., J. Harynuk, and O. Panic, The evolution of comprehensive two-dimensional gas chromatography (GC × GC), *J. Separation Science*, 2004, **27**, 359–379.

Grantham, P.J., J. Posthuma, and K. DeGroot, Variation and significance of the C27 and C28 triterpane content of a North Sea core and various North Sea crude oils, *Advances in Organic*

Geochemistry, A.G. Douglas and J.R. Maxwell (eds.), 1980, Pergamon, Oxford, 29–38.

Hornafius, J.S., D.C. Quigley, and B.P. Luyendyk, The world's most spectacular marine hydrocarbon seeps (Coal Point, Santa Barbara Channel, California): Quantification of emissions, *J. Geophysical Research*, 1999, **104**, 20703–20711.

Hostettler, F.D., R.J. Rosenbauer, T.D. Lorenson, and J. Dougherty, Geochemical characterization of tarballs on beaches along the California coast. Part I — Shallow seepage impacting the Santa Barbara Channel Islands, Santa Cruz, Santa Rosa, and San Miguel, *Organic Geochemistry*, 2004, **35**, 725–746.

Johnson, K.J. and R.E. Synovec, Pattern recognition of jet fuels: Comprehensive GC × GC with ANOVA-based feature selection and principal component analysis, *Chemometrics and Intelligent Laboratory Systems*, 2002, **60**, 225–237.

Johnson, K.J., B.W. Wright, K.H. Jarman, and R.E. Synovec, High-speed peak matching algorithm for retention time alignment of gas chromatographic data for chemometric analysis, *J. Chromatography A*, 2003, **996**, 141–155.

Kaplan, I.R. and W.E. Reed, Chemistry of marine petroleum seeps in relation to exploration and pollution, *Proc. Annual Offshore Tech. Conf.*, 1977, **9**, 425–434.

Kates, M., *The Biochemistry of Archaea (Archaebacteria)*, Chap. 9: Membrane Lipids of Archaea, 1993, Elsevier Science Publishers B.V., 261–295.

Koga, Y., M. Nishihara, H. Morii, and M. Akagawa-Matsushita, Ether polar lipids of methanogenic bacteria: Structures, comparative aspects, and biosyntheses, *Microbiological Reviews*, 1993, **57**, 164–182.

Kvenvolden, K.A. and F.D. Hostettler, Geochemistry of coastal tarballs in southern California — a tribute to I.R. Kaplan, *Special Publication — The Geochemical Society*, **9** (Geochemical Investigations in Earth and Space Science), 2004, 197–209.

Lee, A.L., K.B. Bartle, and A.C. Lewis, A model of peak amplitude enhancement in orthogonal two-dimensional gas chromatography, *Analytical Chemistry*, 2001, **73**, 1330–1335.

Leifer, I., J.R. Boles, B.P. Luyendyk, and J.F. Clark, Transient discharges from marine hydrocarbon seeps: Spatial and temporal variability, *Environmental Geology*, 2004, **46**, 1038–1052.

Liu, Z. and J.B. Phillips, Sensitivity and detection limit enhancement of gas chromatographic detection by thermal modulation, *J. Microcolumn Separation*, 1994, **6**, 229–235.

Liu, Z. and M.L. Lee, Comprehensive two-dimensional separations using microcolumns, *J. Microcolumn Separations*, 2000, **12**, 241–254.

Marriott, P. and R. Kinghorn, Cryogenic solute manipulation in gas chromatography — the longitudinal modulation approach, *Trends in Analytical Chemistry*, 1999, **18**, 114–125.

Micyus, N.J., J.D. McCurry, and J.V. Seeley, Analysis of aromatic compounds in gasoline with flow-switching comprehensive two-dimensional gas chromatography, *J. Chromatography A*, 2005, **1086**, 115–121.

Mikolaj, P.G., Composition of oil from the region of new hydrocarbon upwelling in the Santa Barbara channel, Government Report Announcement (U.S.), 1973, **73**, 137.

Moldowan, J.M., W.K. Seifert, and E.J. Gallegos, Relationship between petroleum composition and depositional environment of petroleum source rocks, *Amer. Assoc. Petroleum Geologists Bull.*, 1985, **69**, 1255–1268.

Nelson, R.K., G.S. Frysinger, G.T. Ventura, R.B. Gaines, C.M. Reddy, and F. Kenig, Using comprehensive two-dimensional gas chromatography to obtain direct evidence of the presence of archaean biomarkers from 2.7 billion year old sediments, 28th International Symposium on Capillary Chromatography and Electrophoresis, Las Vegas, NV, May 2005.

Nelson, R.K., B.S. Kile, D.L. Plata, S.P. Sylva, L. Xu, C.M. Reddy, R.B. Gaines, G.S. Frysinger, and S.E. Reichenbach, Tracking the weathering of an oil spill with comprehensive two-dimensional gas chromatography, *Environmental Forensics*, 2006, **7**, 33–44.

Ni, M., S.E. Reichenbach, A. Visvanathan, J. TerMaat, and E.B. Ledford, Jr. Peak pattern variations related to comprehensive two-dimensional gas chromatography acquisition, *J. Chromatography A*, 2005, **1086**, 165–170.

Orphan, V.J., K.-U. Hinrichs, W. Ussler III, C.K. Paull, L.T. Taylor, S.P. Sylva, J.M. Hayes, and E.F. DeLong, Comparative analysis of methane-oxidizing Archaea and sulfate-reducing bacteria in anoxic marine sediments, *Applied and Environmental Microbiology*, 2001, **67**, 1922–1934.

Peters, K.E., C.C. Walters, and J.M. Moldowan, *The Biomarker Guide. Vol. 1: Biomarkers and Isotopes in the Environment and Human History*, 2nd ed., 2004a, Cambridge University Press, Cambridge, pp 12, 58–64, 80, 252, 308.

Peters, K.E., C.C. Walters, and J.M. Moldowan, *The Biomarker Guide. Vol. 2: Biomarkers and Isotopes in the Petroleum Exploration and Earth History*, 2nd ed., 2004b, Cambridge University Press, Cambridge, pp 497–520, 524–526, 608–619, 625–631.

Phillips, J.B., R.B. Gaines, J. Blomberg, F.W.M. van der Wielen, J.-M. Dimandja, V. Green, J. Granger, D. Patterson, L. Racovalis, H.-J. de Geus, J. de Boer, P. Haglund, J. Lipsky, V. Sinha, and E.B. Ledford, A robust thermal modulator for comprehensive two-dimensional gas chromatography, *J. High Resolution Chromatography*, 1992, **22**, 3–10.

Phillips, J.B. and J. Beens, Comprehensive two-dimensional gas chromatography: A hyphenated method with strong coupling between the two dimensions, *J. Chromatography A*, 1999, **856**, 331–347.

Prazen, B.J., K.J. Johnson, A. Weber, and R.E. Synovec, Two-dimensional gas chromatography and trilinear partial least squares for the quantitative analysis of aromatic and naphthene content in naphtha, *Analytical Chemistry*, 2001, **73**, 5677–5682.

Prince, R.C., D.L. Elmendorf, J.R. Lute, C.S. Hsu, C.E. Haith, J.D. Senius, G.J. Dechert, G.S. Douglas, and E.L. Butler, 17α(H),21β(H)-hopane as a conserved internal marker for estimating the biodegradation of crude oil, *Environmental Science and Technology*, 1994, **38**, 142–145.

Quigley, D., J.S. Hornafius, B.P. Luyendyk, R.D. Francis, and E.C. Bartsch, Temporal variations in the spatial distribution of natural marine hydrocarbon seeps in the Northern Santa Barbara Channel, California, *EOS, Trans., Amer. Geophysical Union, Electronic Supplement*, 1996, **77**, F419.

Quigley, D.C., J.S. Hornafius, B.P. Luyendyk, R.D. Francis, J. Clark, and L. Washburn, Decrease in natural marine hydrocarbon seepage near Coal Oil Point, California, associated with offshore oil production, *Geology*, 1999, **27**, 1047–1050.

Reed, W.E. and I.R. Kaplan, The chemistry of marine petroleum seeps, *J. Geochemical Exploration*, 1977, **7**, 255–293.

Reddy, C.M., T.I. Eglinton, A. Hounshell, H.K. White, L. Xu, R.B. Gaines, and G.S. Frysinger, The West Falmouth oil spill after thirty years: The persistence of petroleum hydrocarbons in marsh sediments, *Environmental Science and Technology*, 2002, **36**, 4754–4760.

Reichenbach, S.E., M. Ni, V. Kottapalli, and A. Visvanathan, Information technologies for comprehensive two-dimensional gas chromatography, *Chemometrics and Intelligent Laboratory Systems*, 2004, **71**, 107–120.

Schoell, M., A.M. McCaffrey, F.J. Fago, and J.M. Moldowan, Carbon isotopic composition of 28,30-bisnorhopanes and other biological markers in a Monterey crude oil, *Geochimica et Cosmochimica Acta*, 1992, **56**, 1391–1399.

Schoenmakers, P.J., J.L.L.M. Oomen, J. Blomberg, W. Genuit, and G. van Velzen, Comparison of comprehensive two-dimensional gas chromatography and gas chromatography — mass spectrometry for the characterization of complex hydrocarbon mixtures, *J. Chromatography A*, 2000, **892**, 29–46.

Seeley, J.V., F. Kramp, and C.J. Hicks, Comprehensive two-dimensional gas chromatography via differential flow modulation, *Analytical Chemistry*, 2000, **72**, 4346–4352.

Seifert, W.K., J.M. Moldowan, G.W. Smith, and E.V. Whitehead, First proof of structure of a C28-pentacyclic triterpane in petroleum, *Nature*, 1978, **271**, 436–437.

Seruto, C., Y. Sapozhnikova, and D. Schlenk, Evaluation of the relationships between biochemical endpoints of PAH exposure and physiological endpoints of reproduction in male California Halibut (*Paralichthys californicus*) exposed to sediments from a natural oil seep, *Marine Environmental Research*, 2005, **60**, 454–465.

Sinha, A.E., B.J. Prazen, C.G. Fraga, and R.E. Synovec, Valve-based comprehensive two-dimensional gas chromatography with time-of-flight mass spectrometric detection: Instrumentation and figures-of-merit, *J. Chromatography A*, 2003, **1019**, 79–87.

Sinha, A.E., J.L. Hope, B.J. Prazen, C.G. Fraga, E.J. Nilsson, and R.E. Synovec, Multivariate selectivity as a metric for evaluating comprehensive two-dimensional gas chromatography-time-of-flight mass spectrometry subjected to chemometric peak deconvolution, *J. Chromatography A*, 2004, **1056**, 145–154.

Sinninghe Damste, J.S., F. Kenig, M.P. Koopmans, J. Koster, S. Schouten, J.M. Hayes, and J.W. de Leeuw, Evidence for gammacerane as an indicator of water column stratification, *Geochimica et Cosmochimica Acta*, 1995, **59**, 1895–1900.

Spies, R.B., P.H. Davis, and D.H. Stuermer, Ecology of a petroleum seep off the California

coast, *Marine Environmental Pollution*, R. Geyer (ed.), 1980, Elsevier, Amsterdam, 229–263.

Stout, S.A., A.D. Uhler, K.J. McCarthy, and S. Emsbo-Mattingly, Chemical Fingerprinting of Hydrocarbons, *Introduction to Environmental Forensics*, B.L. Murphy and R.D. Morrison (eds.), 2002, Academic Press, San Diego, 135–260.

Stout, S.A., A.D. Uhler, and K.J. McCarthy, Middle distillate fingerprinting using drimane-based bicyclic sesquiterpanes, *Environmental Forensics*, 2005, **6**, 241–251.

Stuermer, D.H., R.B. Spies, and P.H. Davis, Toxicity of Santa Barbara seep oil to starfish embryos: Part 1. Hydrocarbon composition of test solutions and field samples, *Marine Environmental Research*, 1981, **5**, 275–286.

Stuermer, D.H., R.B. Spies, P.H. Davis, D.J. Ng, C.J. Morris, and S. Neal, The hydrocarbons in the Isla Vista marine seep environment, *Marine Chemistry*, 1982, **11**, 413–426.

Teal, J.M., J.W. Farrington, K.A. Burns, J.J. Stegeman, B.W. Tripp, B. Woodin, and C. Phinney, The West Falmouth oil spill after 20 years: Fate of fuel oil compounds and effects on animals, *Marine Pollution Bulletin*, 1992, **24**, 607–614.

ten Haven, H.L., J.W. de Leeuw, J.S. Sinninghe Damste, Schenck, S.E. Palmer, and J.E. Zomberge, Application of biological markers in the recognition of palaeo-hypersaline environments, *Lacustrine Petroleum Source Rock*, K. Kelts, A.J. Fleet, and M.R. Talbot (eds.), 1988, Blackwell Publishing, Oxford, **40**, 123–130.

ten Haven, H.L., M. Rohmer, J. Rullkotter, and P. Bisseret, Tetrahymanol, the most likely precursor of gammacerane, occurs ubiquitously in marine sediments, *Geochimica et Cosmochimica Acta*, 1989, **53**, 3073–3079.

van Deursen, M., J. Beens, J. Reijenga, P. Lipman, and C. Cramers, Group-type identification of oil samples using comprehensive two-dimensional gas chromatography coupled to a time-of-flight mass spectrometer (GC × GC-TOF), 2000, **23**, 507–510.

van Stee, L.L.P., J. Beens, R.J.J. Vreuls, and U.A.Th Brinkman, Comprehensive two-dimensional gas chromatography with atomic emission detection and correlation with mass spectrometric detection: Principles and application to petrochemical analysis, *J. Chromatography A*, 2003, **1019**, 89–99.

Vendeuvre, C., F. Bertoncini, L. Duval, J.-L. Duplan, D. Thiebaut, and M.-C. Hennion, Comparison of conventional gas chromatography and comprehensive two-dimensional gas chromatography for the detailed analysis of petrochemical samples, *J. Chromatography A*, 2004, **1056**, 155–162.

Vendeuvre, C., R. Ruiz-Guerro, F. Bertoncini, L. Duval, D. Thiebaut, and M.-C. Hennion, Characterisation of middle-distillates by comprehensive two-dimensional gas chromatography (GC × GC): A powerful alternative for performing various standard analysis of middle-distillates, *J. Chromatography A*, 2005a, **1086**, 21–28.

Vendeuvre, C., F. Bertoncini, D. Espinat, D. Thiebaut, and M.-C. Hennion, Multidimensional gas chromatography for the detailed PIONA analysis of heavy naphtha: Hyphenation of an olefin trap to comprehensive two-dimensional gas chromatography, *J. Chromatography A*, 2005b, **1090**, 116–125.

Venkatramani, C.J. and J.B. Phillips, Comprehensive two-dimensional gas chromatography applied to the analysis of complex mixtures, *J. Microcolumn Separations*, 1993, **5**, 511–516.

Volkman, J.K., R. Alexander, R.I. Kagi, S.J. Rowland, and P.N. Sheppard, Biodegradation of aromatic compounds in crude oils from the Barrow Sub-basin of Western Australia, *Organic Geochemistry*, 1984, **6**, 619–632.

Volkman, J.K., Sterols and other triterpenoids: Source specificity and evolution of biosynthetic pathways, *Organic Geochemistry*, 2005, **36**, 139–159.

Wang, F.C-Y., W.K. Robbins, and M.A. Greaney, Speciation of nitrogen-containing compounds in diesel fuel by comprehensive two-dimensional gas chromatography, *J. Separation Science*, 2004, **27**, 468–472.

Wang, Z., C. Yang, M. Fingas, B. Hollebone, X. Peng, A.B. Hansen, and J.H. Christensen, Characterization, weathering, and application of sesquiterpanes to source identification of spilled lighter petroleum products, *Environmental Science and Technology*, 2005, **39**, 8700–8707.

Washburn, L., J.S. Hornafius, B.P. Luyendyk, J.F. Clark, D. Quigley, and D.F. Francis, Dispersal of hydrocarbon gas plumes in the Northern Santa Barbara Channel, CA; *EOS, Trans., Amer. Geophysical Union, Electronic Supplement*, 1996, **77**, F419.

Woese, C.R. and G.E. Fox, Phylogenetic structure of the prokaryotic domain: The primary kingdoms, *Proc. National Academy of Sciences*, 1977, **74**, 5088–5090.

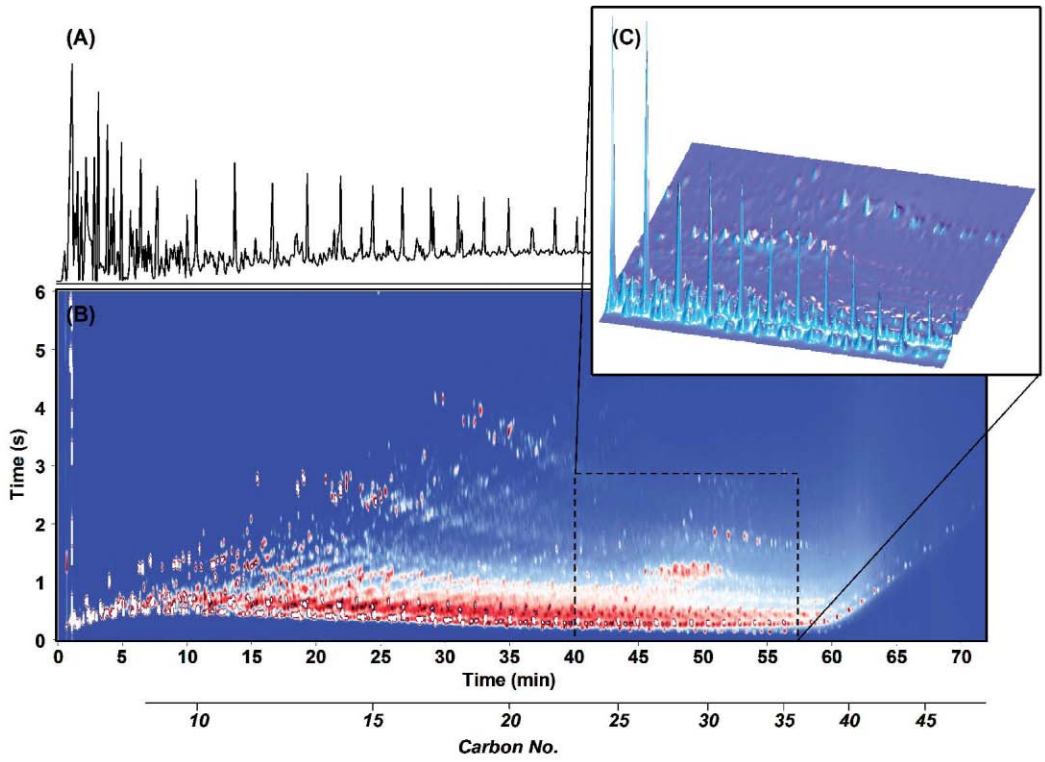

Figure 5-3 Chromatograms of *Exxon Valdez* cargo oil: (A) One-dimensional gas chromatogram using a nonpolar 100% polydimethylsiloxane stationary phase; (B) GC × GC volatility-by-polarity interpolated color contour plot. The first dimension is a separation using a nonpolar 100% polydimethylsiloxane stationary phase and the second dimension is a separation using a polar 50% phenyl polysilphenylene stationary phase; (C) a small portion of the GC × GC chromatogram visualized as a mountain plot. The mountain plot is excellent for visualizing relative differences among neighboring peaks.

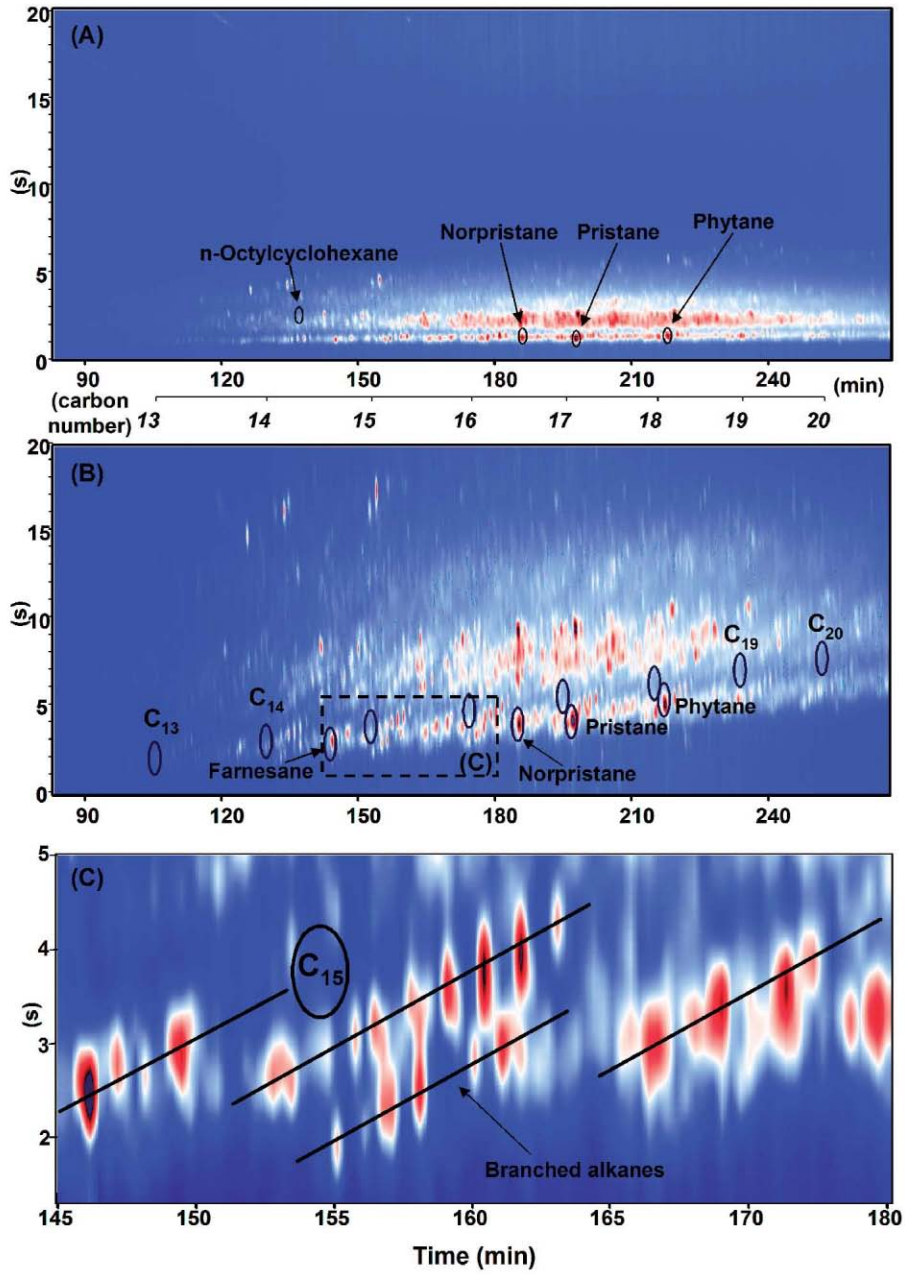

Figure 5-6 Effect of changing the second-dimension stationary phase on the separation of nonpolar saturates: (A) GC × GC chromatogram of the saturates fraction of a sediment extract using a polar second-dimension 14% cyanopropylphenyl polysiloxane stationary phase; (B) GC × GC chromatogram of the same saturates fraction using a chiral γ-cyclodextrin second-dimension stationary phase. The expected positions of the *n*-C_{13} to *n*-C_{20} alkanes are marked with circles. The region inside the dotted lines is expanded in (C); (C) expanded region showing expected position of *n*-C_{15} and location of branched alkane bands. Reprinted with permission from Frysinger et al., 2003. Copyright 2003, American Chemical Society.

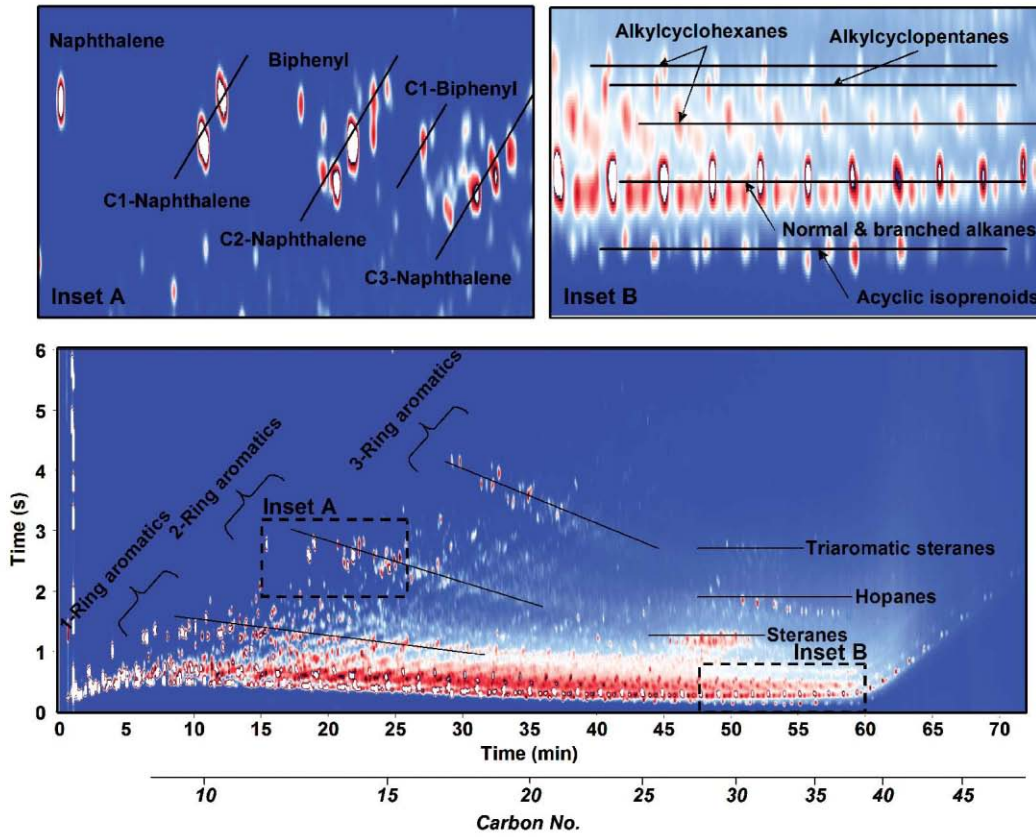

Figure 5-7 Location of petroleum chemical classes on a volatility-by-polarity GC × GC chromatogram. Nonpolar alkanes are located at the bottom, with one- and multiring aromatics further up the *y*-axis as their polarity increases. Inset A: naphthalene region showing bands of alkyl-substituted naphthalenes and biphenyls; Inset B: nonpolar region showing high-resolution separations of higher boiling (C_{28}+) acyclic isoprenoids, normal and branched alkanes, and cyclic alkanes.

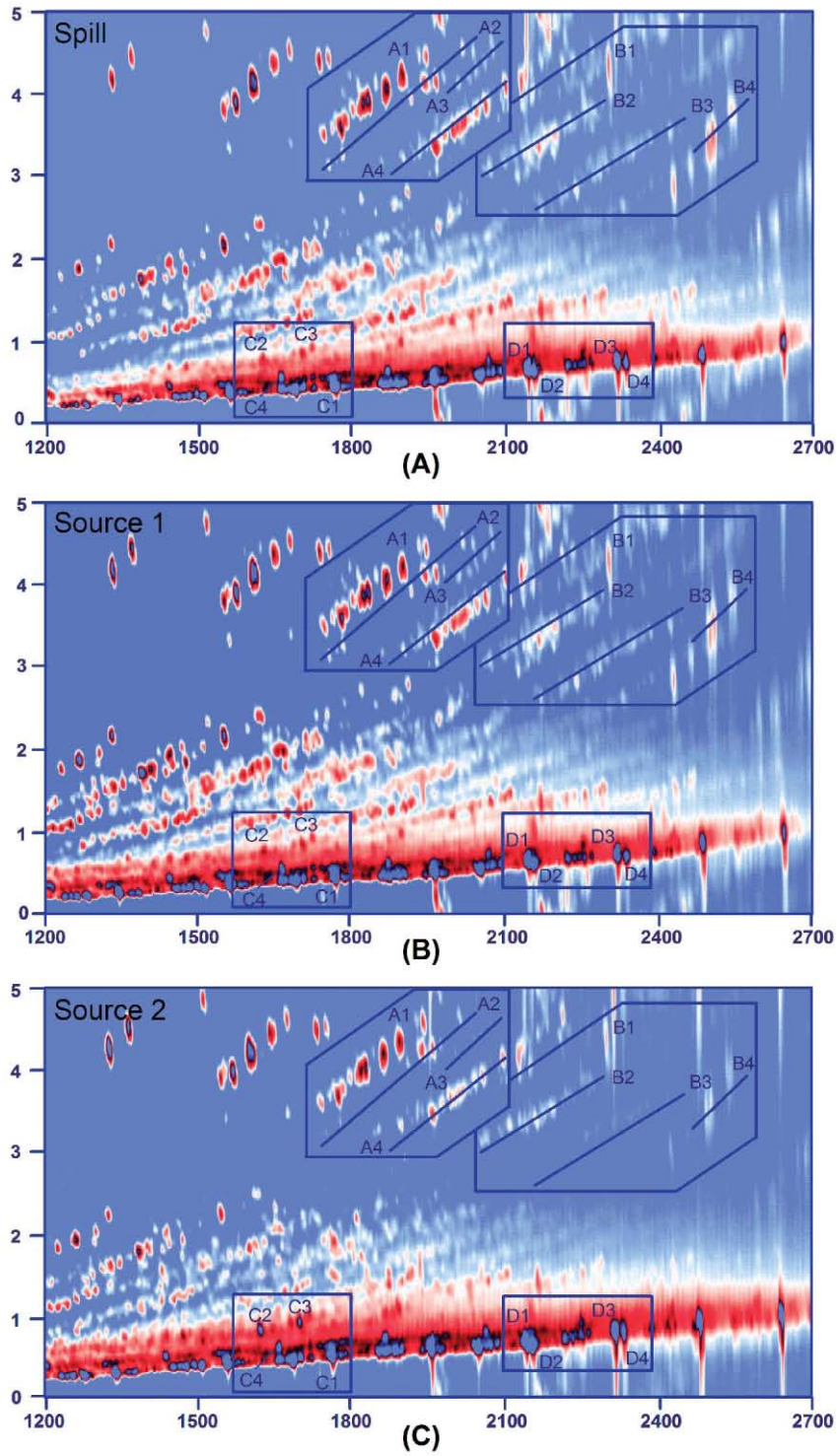

Figure 5-8 Portion of a volatility-by-polarity GC × GC-FID chromatogram from each of the three samples compared: (a) spill; (b) and (c) potential spill sources. Both axes are in seconds. The boxes contain chemical families and individual compounds used to qualitatively and quantitatively compare two potential source samples with the spill samples. The first column separation shown along the *x*-axis was accomplished with a nonpolar 5% phenylmethylsiloxane stationary phase. The second column separation shown along the *y*-axis was accomplished with a polar polyethylene glycol/siloxane copolymer stationary phase. Reprinted with permission from Gaines et al., 1999. Copyright 1999, American Chemical Society.

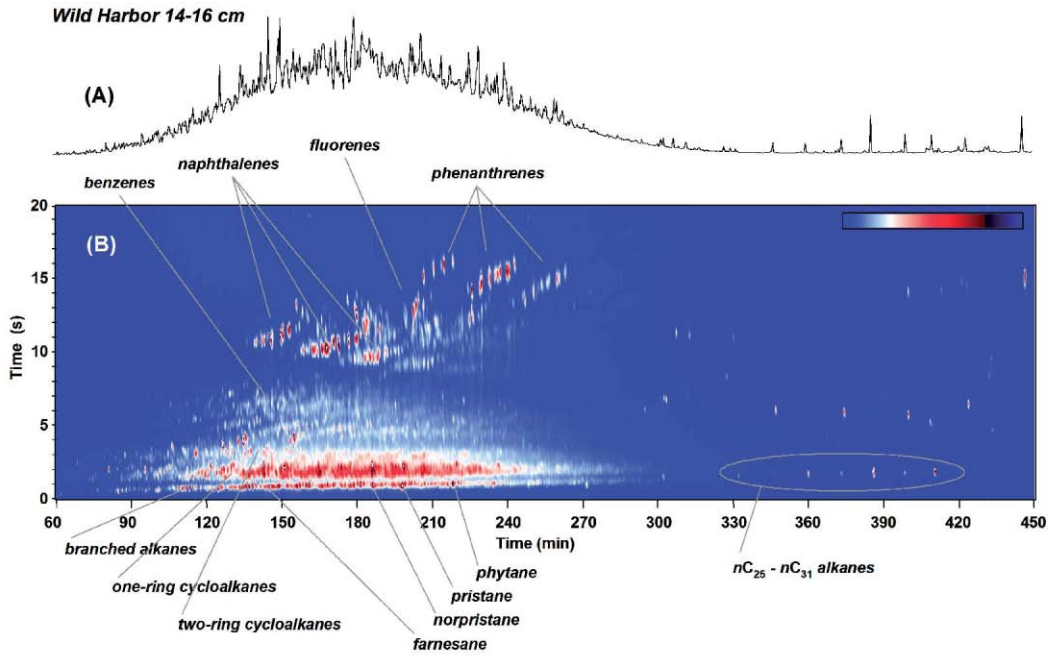

Figure 5-12 Chromatograms of a Wild Harbor sediment extract, Aug. 2000: (A) Conventional one-dimensional gas chromatogram. The separation was accomplished using a nonpolar polydimethylsiloxane stationary phase; (B) volatility-by-polarity GC × GC chromatogram. The first column separation along the *x*-axis was accomplished using a nonpolar polydimethylsiloxane stationary phase. The second column separation was accomplished using a polar 14%-cyanopropylphenyl polysiloxane stationary phase. Reprinted with permission from Reddy et al., 2002. Copyright 2002, American Chemical Society.

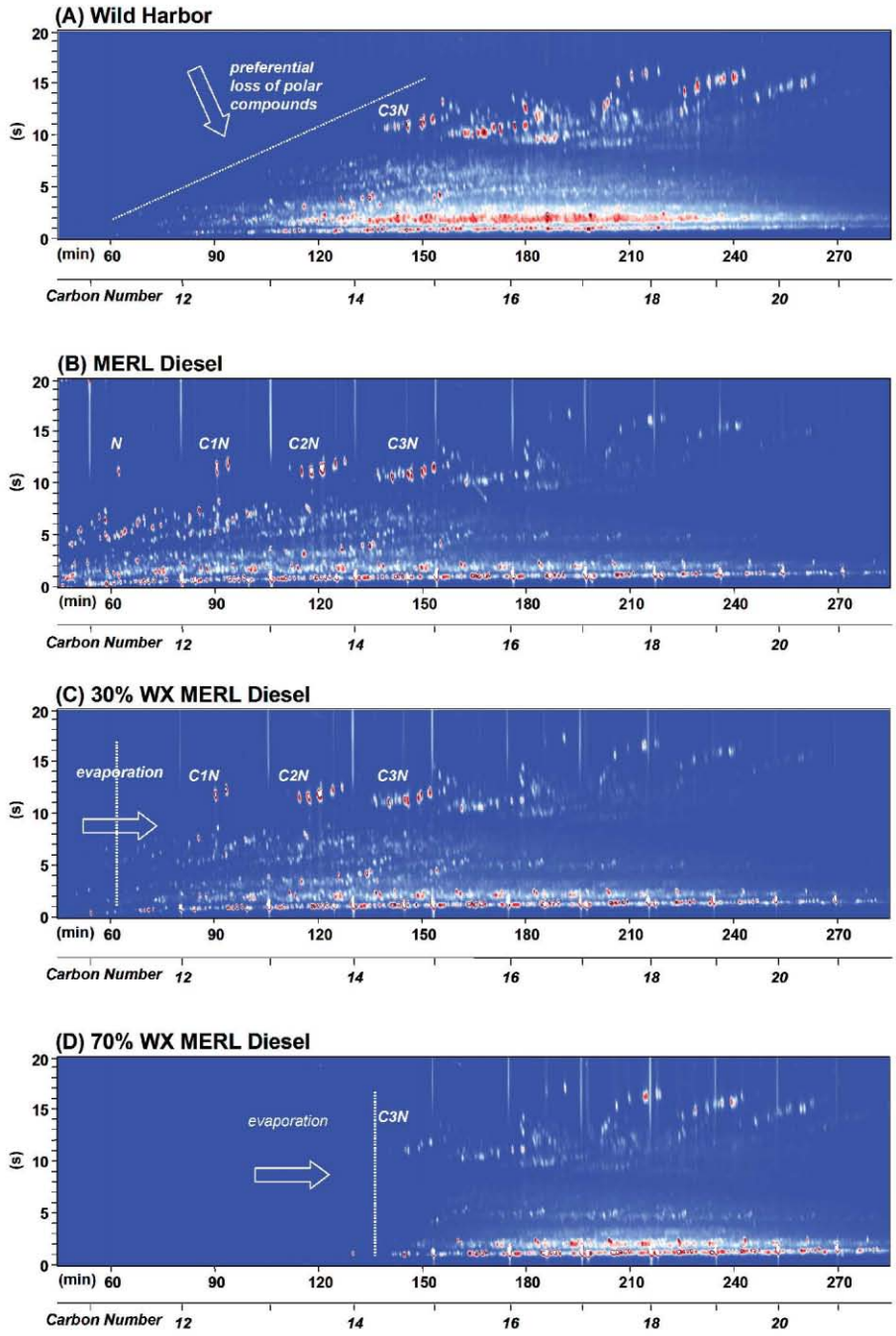

Figure 5-13 Comparison of Wild Harbor sediment extract with weathered MERL oil: (A) Enlarged volatility-by-polarity GC × GC chromatogram of Wild Harbor extract, Aug. 2000 (as in Figure 5-12); (B) neat MERL oil; (C) 30% by mass weathered (WX) MERL oil; (D) 70% by mass weathered (WX) MERL oil. The first column separation along the *x*-axis was accomplished using a nonpolar polydimethylsiloxane stationary phase. The second column separation was accomplished using a polar 14%-cyanopropylphenyl polysiloxane stationary phase. Weathering experiments were performed in a hood where neat MERL oil was allowed to evaporate until the desired mass loss was achieved. The background is blue. Peak intensity is scaled from white, to red, and then to blue (most intense). Compound abbreviations: (N) naphthalene; (C1N) C_1-naphthalenes; (C2N) C_2-naphthalenes; (C3N) C_3-naphthalenes. Reprinted with permission from Reddy et al., 2002. Copyright 2002, American Chemical Society.

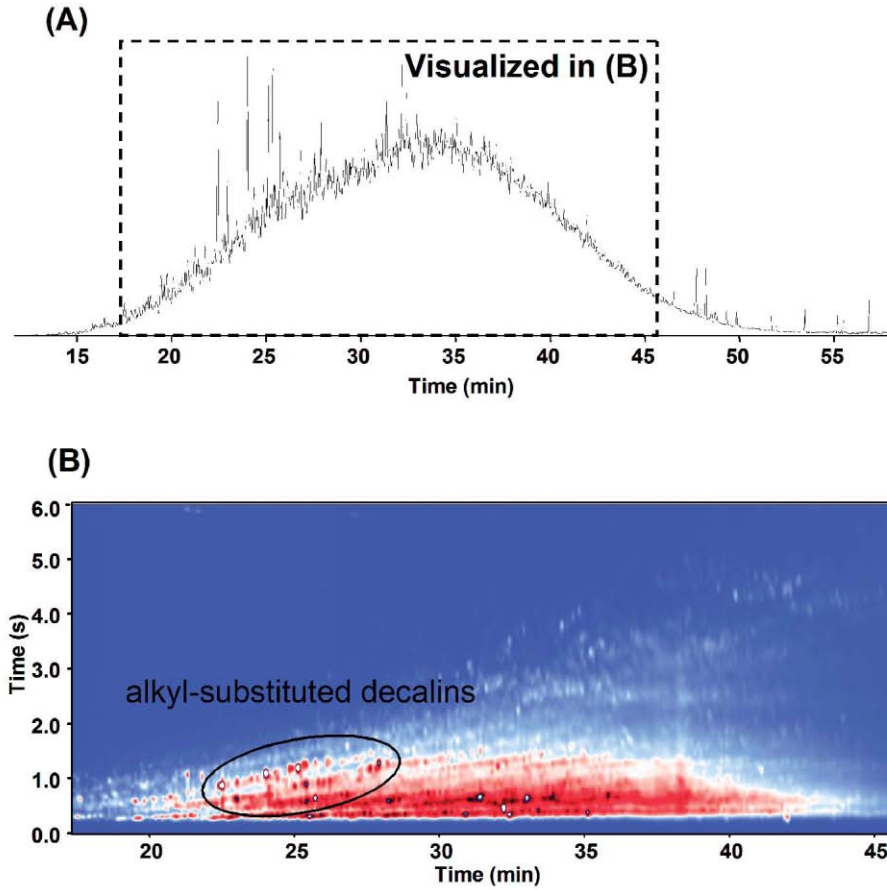

Figure 5-15 Chromatograms of the sediment extract taken from Winsor Cove in 2002 approximately 30 years after being contaminated with No. 2 fuel oil: (A) one-dimensional gas chromatogram showing UCM and the region of the chromatogram visualized in (B). The separation was accomplished using a polydimethylsiloxane stationary phase; (B) volatility-by-polarity GC × GC-FID chromatogram showing the region containing the target compounds. The first-column separation shown along the *x*-axis was accomplished with a polydimethylsiloxane stationary phase. The second-column separation shown along the *y*-axis was accomplished with a 50%-phenylpolysilphenylene-siloxane stationary phase.

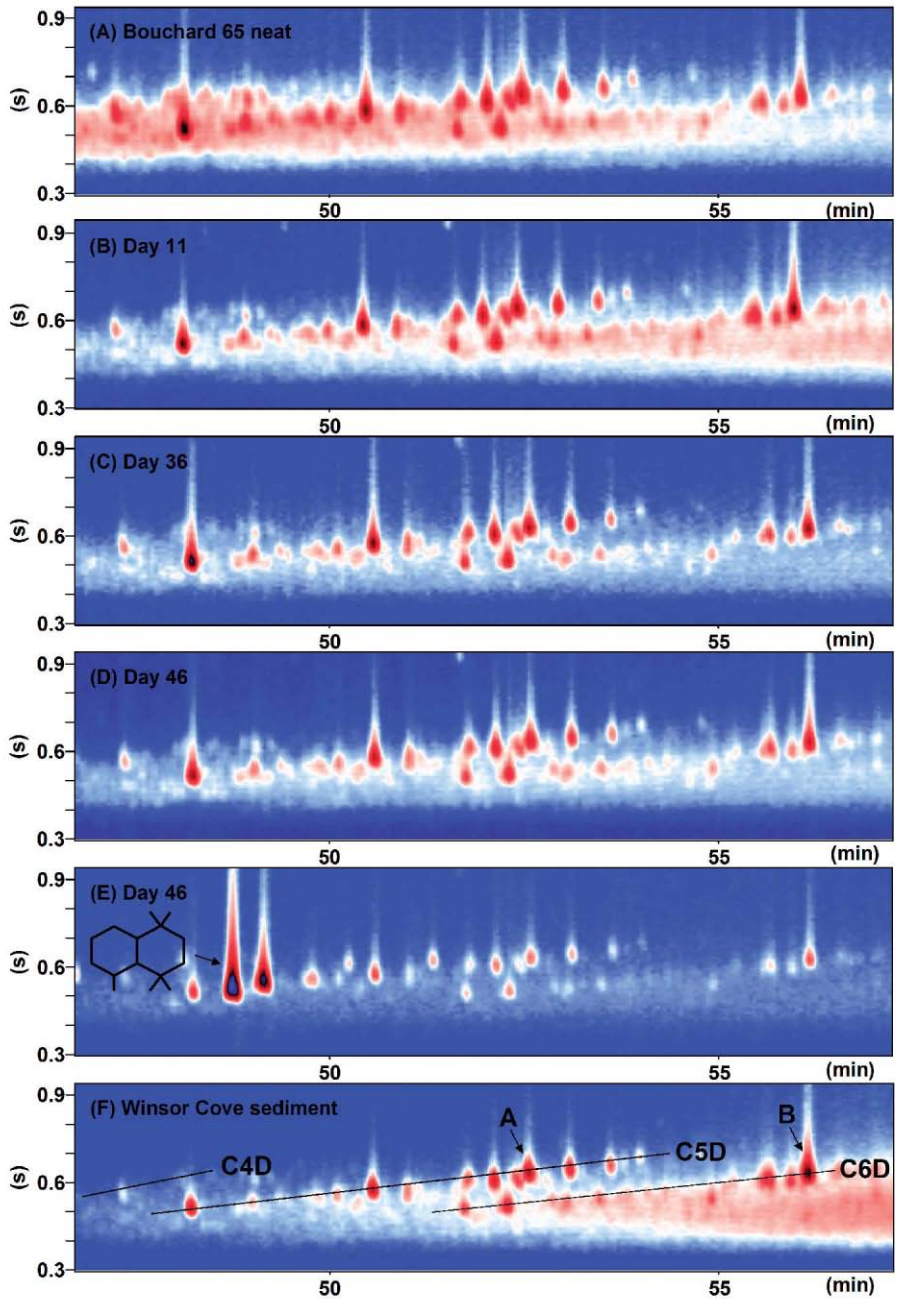

Figure 5-18 Volatility-by-polarity GC × GC m/z = 123 extracted ion chromatographs of *Bouchard 65* incubation sediment extracts showing the C_4- to C_6-decalin region: (A) neat *Bouchard 65* fuel oil; (B) day 11; (C) day 36; (D) day 46; (E) day 46 spiked with cis- and trans-1,1,4,4,6-pentamethyldecalin standard; (F) Winsor Cove sediment extract showing the bands of peaks containing C_4-decalins (C4D), C_5-decalins (C5D), C_6-decalins (C6D), and location of 8β(H)-drimane (A) and 8β(H)-homodrimane (B) whose structures are given in Figure 5-16. The first-column separation shown along the *x*-axis was accomplished with a nonpolar polydimethylsiloxane stationary phase. The second-column separation shown along the *y*-axis was accomplished with a polar 50%-phenylpolysilphenylene-polysiloxane stationary phase.

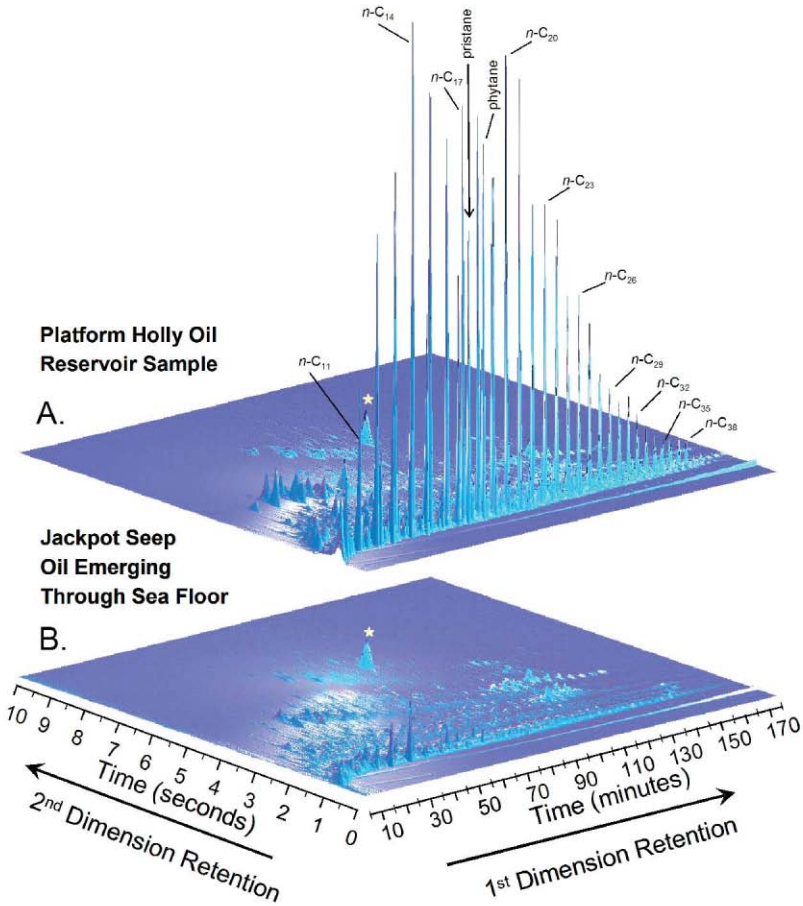

Figure 5-22 Volatility-by-polarity GC × GC chromatogram of (A) reservoir crude oil from platform Holly, Santa Barbara Channel, California, and (B) oil stringer emerging through the sea floor collected at the Jackpot seep field, Santa Barbara Channel, California. The first-column separation shown along the *x*-axis was accomplished with a nonpolar polydimethylsiloxane stationary phase. The second-column separation shown along the *y*-axis was accomplished with a polar 50%-phenylpolysilphenylene-siloxane stationary phase. A star on each chromatogram indicates the position of the internal standard dodecahydrotriphenylene (DDTP). The distinct difference in *n*-alkane content between the two samples is evident in this figure.

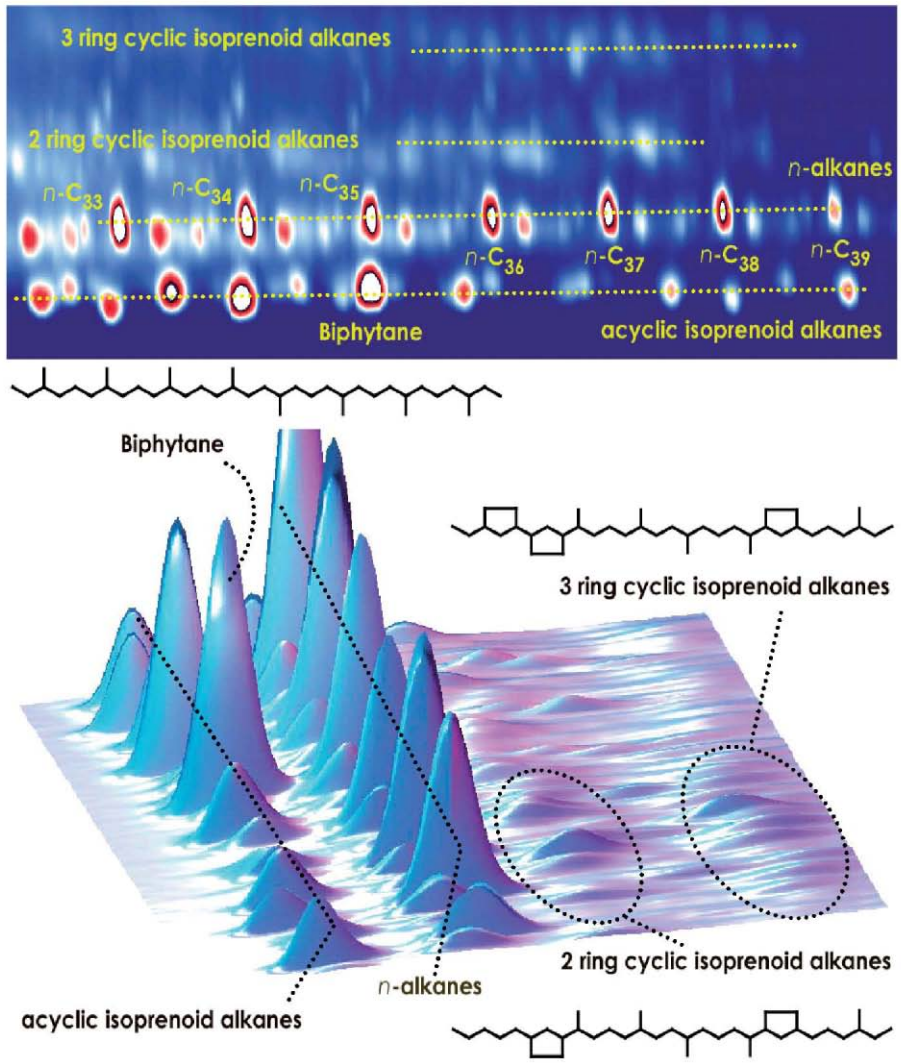

Figure 5-23 Partial volatility-by-polarity GC × GC chromatogram of the platform Holly produced crude oil showing peaks in the vicinity of n-C_{33} through n-C_{39}. The location of high-molecular-weight isoprenoid alkanes (both acyclic and cyclic), thought to be biomarkers of Archaean membrane lipids, are indicated along with some representative molecular structures.

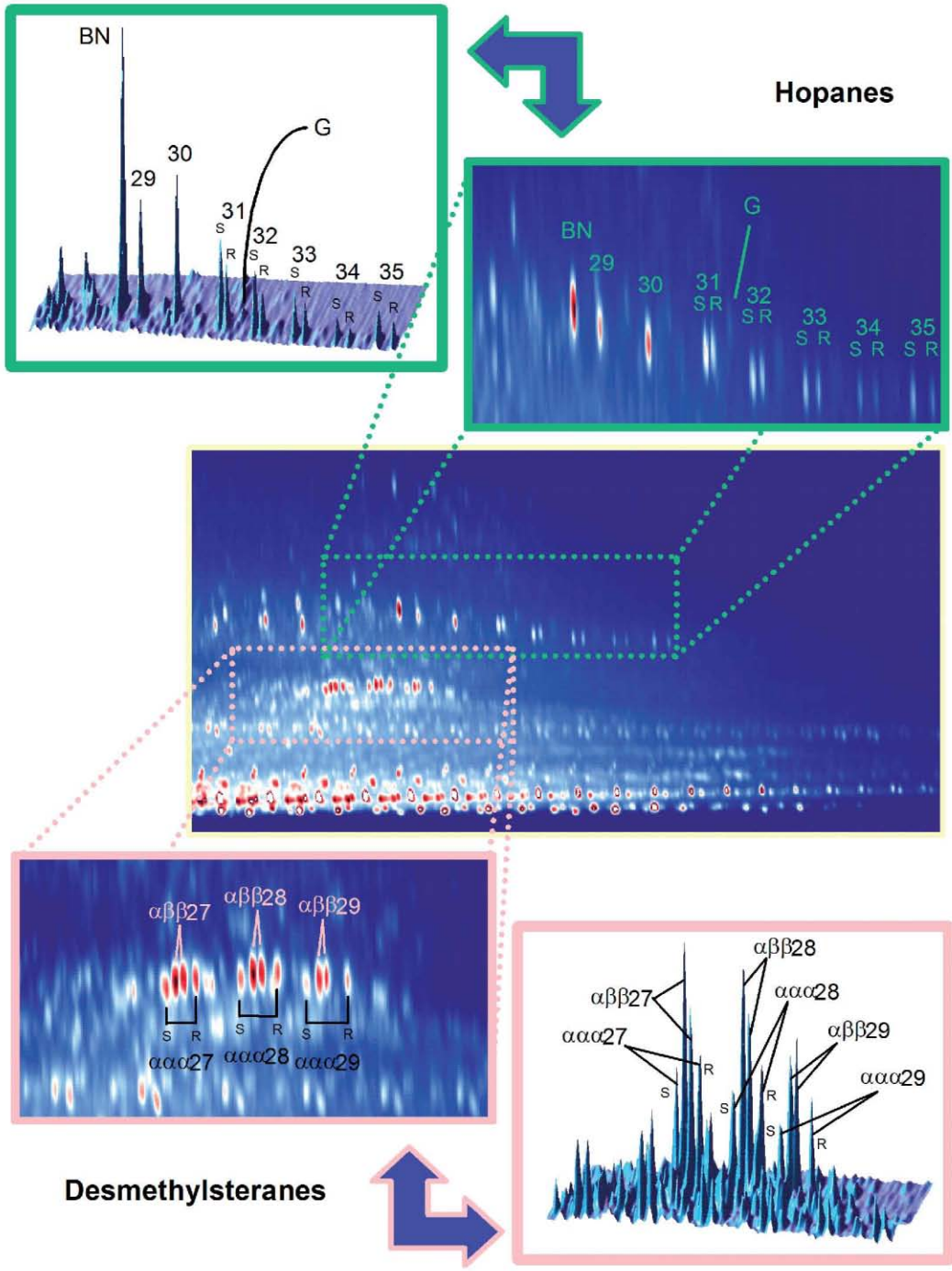

Figure 5-24 Partial volatility-by-polarity GC × GC chromatogram of the platform Holly reservoir crude oil showing peaks in the vicinity of the sterane and desmethylsterane biomarkers. Identification of labeled peaks is found in Table 5-1.